# Optimizing Cucumber Fruit Metabolomics under Elevated $CO_2$ and High-Temperature Stress in Protected Horticulture

Xian Du , Yang Song , Lu Pan , Shimao Cui *

Posted Date: 26 November 2024

doi: 10.20944/preprints202411.1977.v1

Keywords: high temperature;$CO_2$; cucumber fruit; physiology; metabolomics

*Article*

# Optimizing Cucumber Fruit Metabolomics under Elevated $CO_2$ and High-Temperature Stress in Protected Horticulture

**Xian Du, Yang Song, Lu Pan and Shimao Cui ***

College of Horticulture and Plant Protection, Inner Mongolia Agricultural University, Hohhot 010018, China
* Correspondence: cuishimao@sina.com

**Abstract:** Elevated carbon dioxide concentrations can mitigate significant threats posed by high-temperature stress to cucumber fruit yield and quality during summer. To investigate the potential metabolic mechanisms, this study employed untargeted metabolomics methods to analyze the effects of varying temperatures and carbon dioxide concentrations on the metabolomic profiles of cucumber fruits. Under high-temperature stress, elevated carbon dioxide concentrations altered 27 differential metabolites, including tyramine, xylitol, linolenic acid, L-asparagine, α-linolenic acid, and L-phenylalanine. These alterations are associated with the metabolic pathways of alanine, aspartate, glutamate, glutathione, glyoxylate, and dicarboxylic acids. Compared to the addition of carbon dioxide at normal temperatures, elevated carbon dioxide at high temperatures modified 38 differential metabolites, including vitamin B6, L-citrulline, inositol, L-aspartic acid, sucrose, and palmitic acid. These modifications were linked to the galactose metabolic pathway and the zeatin and arginine biosynthetic pathways. The accumulation of cysteine, glutamic acid, and glycine is essential for the formation of antioxidant glutathione; thus, cucumber fruits with higher amino acid content exhibit an enhanced capacity to withstand severe high-temperature stress. Under high-temperature conditions, elevated carbon dioxide adds complexity to the changes in differential metabolites within cucumber fruits. These fruits accumulate sugars, organic acids, and amino acids through the galactose metabolism pathway (map00052), the arginine biosynthesis pathway (map00220), and the glutamate synthesis pathway (map00250), thereby improving their heat resistance.

**Keywords:** high temperature;$CO_2$; cucumber fruit; physiology; metabolomics

## 1. Introduction

Amidst the ongoing global climate change, protected horticulture is essential to ensure food security and promote sustainable agriculture. While long-term climate change affects the cultivated land area and cropping systems, short-term abiotic stresses faced by horticultural crops during their fruiting period frequently result in seasonal yield reductions or total crop failure, a leading cause of global horticultural crop loss.[1,2].

Cucumber (*Cucumis sativus* L.) is one of the most widely cultivated and economically significant vegetables worldwide[3]. High temperatures harm cucumber production in greenhouses, where optimal photosynthesis occurs between 25-33 °C[4]. Open field temperatures can exceed 38 °C during summer, while greenhouse temperatures can exceed 45 °C. Prolonged heat stress adversely affects cucumber transpiration, respiration, and photosynthesis, reducing growth and yield and negatively impacting the content of organic acids, vitamin C, soluble protein, and soluble sugars in cucumber fruits[5]. Additionally, the enclosed structure of greenhouses restricts internal and external gas exchange. Although atmospheric $CO_2$ levels increase annually, they remain at 380 μmol/mol, only 30% of the optimal level for plant photosynthesis[6]. This $CO_2$ deficiency directly impedes photosynthesis and the accumulation of nutrients in leaves. According to the model proposed by Schapendonk et al.[7], greenhouse $CO_2$ deficiency could decrease cucumber net assimilation by 15% and long-term yields by 11%. Our previous studies have demonstrated that under high temperature

 doi:10.20944/preprints202411.1977.v1



conditions (45 °C), increasing $CO_2$ levels can significantly enhance the net photosynthetic rate of cucumber during the photosynthetic 'noon break' period, expand the suitable temperature range for photosynthesis, promote leaf growth, delay plant senescence, and increase biomass production, as well as the sugar and organic acid content in cucumber fruits[8]. Furthermore, elevated $CO_2$ levels help regulate the expression of differential proteins associated with various biological processes[9]. While considerable knowledge exists about the role of elevated $CO_2$ in alleviating the detrimental effects of high-temperature stress on plants, there is an urgent need for research to elucidate the impact of elevated $CO_2$ in conjunction with high-temperature stress on horticultural plant metabolites. This understanding is critical in light of the pressing challenges of climate change and food security.

Recently, metabolomics technology has been extensively used to analyze metabolic networks associated with plant growth, development, and responses to abiotic stress[10]. Increased soluble sugars and amino acid concentrations are recognized as generalized heat response mechanisms in various plant species. The accumulation of primary metabolites, such as carbohydrates, enhances the stability of proteins and the bilayer structure of the cell membrane[11]. Elevated levels of pipecolic acid, oleic acid, and raffinose may signify that these metabolites serve as first-line defense mechanisms for cucumbers against heat stress[12,13]. The ascorbic acid (ASA) accumulation in tomato fruits has improved fruit quality and alleviated abiotic stress[14]. Ecometabolomic studies indicate that the metabolites that increase most significantly in plants under elevated atmospheric $CO_2$ levels are terpenes and soluble sugars, particularly the monosaccharides galactose, glucose, and fructose. This suggests that increases in newly photosynthesized carbon trigger the immediate accumulation of photosynthetic products[15]. Furthermore, elevated $CO_2$ levels facilitate the accumulation of carbohydrates, 1,2,3-trihydroxy benzene, pyrocatechol, glutamate, and L-gluconolactone, enabling cucumber seedlings to adapt to severe drought conditions[16].

The commercial value of cucumbers is closely linked to the quality of the fruit, which is directly influenced by the growth environment. Currently, most studies utilizing artificial climate chambers, pot experiments, and controlled indoor environments have focused on the individual effects of carbon dioxide and elevated temperatures on various crops' phenology, physiology, and biochemistry [17–20]. However, there have been no prior reports on metabolomics investigations of cucumber fruit subjected to elevated $CO_2$ and high-temperature stress. This study aimed to elucidate the response mechanisms of cucumber fruit metabolomics under elevated $CO_2$ and high-temperature stress and explore the potential benefits of elevated $CO_2$ in mitigating the adverse effects of high temperatures. This study included physiological analysis, assessing factors such as fruit size, number of fruits per plant, weight of individual fruits, yield per plant, total number of fruits, total weight of fruits, ascorbic acid content, nitrite content, soluble sugar content, and starch content, alongside metabolomics analysis utilizing ultra-high performance liquid chromatography quadrupole time-of-flight mass spectrometry (UHPLC-Q-TOF MS). Special attention was given to the changes in differential metabolites and metabolic pathways under varying treatment conditions and how these alterations impact the quality of cucumber fruits. The findings of this research contribute valuable insights into the environmental adaptability of protected horticultural crops and the application of carbon dioxide fertilization technology, providing a theoretical foundation for utilizing exogenous metabolites to enhance the heat resistance of cucumbers.

## 2. Materials and Methods

### *2.1. Plant Material, Growth Conditions, and Experimental Design*

The experiment was conducted at the Free Air Temperature Elevation Facility (FATE) of Inner Mongolia Agricultural University, located in the Saihan District of Hohhot, Inner Mongolia Autonomous Region, China (111°41′E, 40°48′N). The greenhouse measures 45 m in length, 7.5 m in width, and 4.2 m in height at the ridge. The test material was cucumber (Cucumis sativus L., 'Jinyou No. 35') obtained from the Tianjin Kernel Cucumber Research Institute in Tianjin. This variety is classified as a North China-type cucumber characterized by its robust parthenocarpy, rapid fruit

 doi:10.20944/preprints202411.1977.v1



growth rate, and resistance to downy mildew, powdery mildew, and fusarium wilt. It has exhibited exceptional performance in protected cultivation across northern China. Uniformly germinated seeds were chosen and sown in black plastic seedling pots (10 cm in diameter and 9 cm in height) filled with a mixture of peat, vermiculite, and perlite in a volume ratio of 3:1:1. They were subsequently placed in a nursery garden. Following the emergence of four to five true leaves, seedlings exhibiting robust main stems, well-developed root systems, and consistent growth were selected for transplantation into the greenhouse for soil cultivation. Before transplantation, uniform measurements of the greenhouse soil indices were taken: alkali hydrolyzable nitrogen content was 41.3 mg/kg, available phosphorus content was 13.5 mg/kg, available potassium content was 123.7 mg/kg, organic matter content was 11.9 g/kg, conductivity was 516.7 ms/cm, and pH was 7.42. The experiment was designed as a randomized complete block design, comprising control and three treatments: the control treatment maintained a normal temperature of 25 to 35 °C with an ambient $CO_2$ concentration of 400±20 μmol/mol (FC); the second treatment maintained high temperatures of 35 to 45 °C with an ambient $CO_2$ concentration of 400±20 μmol/mol (FT1); the third treatment involved a normal temperature of 25 to 35 °C with an elevated $CO_2$ concentration of 1200±20 μmol/mol (FT2); and the fourth treatment involved high temperatures of 35 to 45 °C with an elevated $CO_2$ concentration of 1200±20 μmol/mol (FT3).

Three replicates were established, each containing 12 cucumber seedlings, resulting in 36 biological replicates per treatment (12 seedlings × 3 replicates). Each treatment area measured 16.5 $m^2$, and cultivation was conducted in a ridge double-row strip mode, with row spacing of 50 cm and plant spacing of 30 cm. The treatments were closed and independent of one another. A drip irrigation belt was employed for uniform irrigation. Throughout the experiment, the soil water content for each treatment was maintained at 70 to 80% of the maximum water holding capacity in the field. The greenhouse experiment was conducted from May to July during the summer (based on the local standard for seasonal division in the Inner Mongolia Autonomous Region, defined as an average temperature exceeding 20 °C for 5 consecutive days). After the initial flowering stage of the cucumber, throughout the fruiting period ( 35 days ), the FT2 and FT3 treatments were enriched with $CO_2$ at a concentration of 1200 ± 20 μmol/mol, while the FC and FT1 treatments were maintained at an ambient $CO_2$ level of approximately 400 μmol/mol. $CO_2$ enrichment occurred daily from 7:00 to 12:00 a.m. for a duration of 5 hours. $CO_2$ was supplied from a compressed gas cylinder, controlled by a solenoid valve, and was automatically injected into the greenhouse to sustain the target concentration. The concentration was monitored using a $CO_2$ measuring instrument (TESTO 535; Germany). The $CO_2$-enriched treatment group was ensured to maintain a uniform $CO_2$ concentration throughout the experiment. Other environmental parameters and agronomic management practices were consistent, except for temperature and $CO_2$ concentration variations.

### *2.2. Measurements of Environmental Factors, Morphological and Physiological Parameters*

Every day, from 7 a.m. to 5 p.m., the RC-4HC temperature and humidity recorder (Jingchuang Electric Company, Jiangsu) and the illuminance meter (Luge Technology Co., Ltd., Hangzhou) continuously measured temperature, humidity, and light intensity in the greenhouse. The $CO_2$ measurement instrument (TESTO 535, Germany) detected $CO_2$ concentration in each treatment during the test period. Diurnal variations in greenhouse environmental factors were analyzed under different treatments. The quality identification period for fruit and vegetable products is contingent upon their optimal edible or processing maturity, with cucumbers being suitable for harvest at the tender stage of fruit development. The sampling method adhered to the Chinese National Standard Sample for Fresh Fruits and Vegetables (GB 88555-88). Following the commencement of the test, the total number and weight of cucumber fruits were recorded according to the commercial standard throughout the fruiting period ( 35 days ). Measurements of the length and diameter of the cucumber fruits were taken, and calculations were made for the number of fruits per plant, the weight of each fruit, and the yield per plant. At 21 days after the initiation of treatment (full fruit period), eight cucumber plants were randomly selected from each treatment group at 10 a.m. The premarked cucumber fruits developed for 14 days following flowering were harvested from the area near the

 doi:10.20944/preprints202411.1977.v1



third layer of functional leaves. Consistent attention was paid to the fruit's position, size, and maturity during sampling. The contents of soluble sugar, starch, ascorbic acid, and nitrite were subsequently determined. The soluble sugar content of the fruits was measured using anthrone sulfuric acid colorimetry[21], while the starch content was assessed through perchloric acid hydrolysis and anthrone colorimetry[22]. The ascorbic acid (vitamin C) content was determined using the method specified in China's national standard for analyzing vitamin C in fruits and vegetables (GB6195-86), which employs the colorimetric method. Using the colorimetric method, nitrite levels were assessed according to China's national standard for determining nitrite and nitrate content in fruits, vegetables, and related products (GB/T15401-1994). The test kit was purchased from the Nanjing Jiancheng Bioengineering Institute (Nanjing, China).

Morphological and physiological parameter data were expressed as mean ± standard deviation (SD). Statistical analysis was performed using SPSS 22.0 (IBM SPSS Statistics 22.0, USA), including one-way and two-way ANOVA. Before variance analysis, the processed data's normal distribution and homogeneity of variance were evaluated. In cases where the data did not meet the criteria for normal distribution and homogeneity of variance, the Scheirer-Ray-Hare rank-based test was employed. For significant results from variance analysis, the Tukey test was utilized to compare significant differences between treatments at a significance level of $P < 0.05$. Graphical representations were created using GraphPad Prism 9.0.

### *2.3. Preparation of Samples for UHPLC-Q-TOF MS and Data Processing*

At 21 days after the initiation of treatment (full fruit period), eight cucumber plants were randomly selected from each treatment group at 10 a.m. The premarked cucumber fruits developed for 14 days following flowering were harvested from the area near the third layer of functional leaves. Careful attention was given to the fruit's position, size, and maturity during sampling for metabolomic analysis. Following independent sampling, the fruits were immediately frozen in liquid nitrogen. After 20 minutes, they were transferred to an ultralow-temperature refrigerator for preservation.

Each biological replicate sample was ground in liquid nitrogen. Approximately 80 mg of each sample was weighed, and 1 ml of a methanol/acetonitrile/water solution (2:2:1, v/v) was added. The samples were vortex mixed and subjected to ultrasonic crushing at low temperature for 30 minutes, repeated twice. They were then incubated at -20 °C for 1 hour to precipitate proteins, followed by centrifugation at 13,000 rpm at 4 °C for 15 minutes. The supernatant was lyophilized and stored at -80 °C for metabolomic analysis of cucumber fruits. Samples were mixed in equal amounts to prepare quality control (QC) samples. These QC samples were utilized to assess instrument status before injection, ensure equilibrium in the chromatography mass spectrometry system, and evaluate system stability throughout the experiment.

The UHPLC-Q-TOF MS analysis was conducted using a UHPLC system (1290 Infinity LC, Agilent Technologies, USA) equipped with a UPLC BEH amide column (1.7 μm, 2.1 mm × 100 mm, Waters, USA) coupled to a Triple TOF 5600 (Q-TOF, AB Sciex, USA).

Chromatographic conditions for HILIC separation involved analyzing the samples with a 2.1 mm × 100 mm ACQUIY UPLC BEH 1.7 μm column (Waters, Ireland) at a column temperature of 25 °C and a flow rate of 0.3 ml/min. The injection volume was set at 2 μL. In both positive and negative modes of ESI, the mobile phase consisted of A = 25 mM ammonium acetate, 25 mM ammonium hydroxide in water and B = acetonitrile. The gradient elution procedure was as follows: the gradient commenced at 95% B for 1 min, then linearly decreased to 65% over 13 min, subsequently reduced to 40% over 2 min and maintained for 2 min before increasing back to 95% in 0.1 min. A 5-minute re-equilibration period was employed at 95%. During the analysis, the samples were placed in an automatic sampler at 4 °C. Continuous sampling was conducted randomly to mitigate the effects of fluctuations in the instrument's detection signal. Quality control (QC) samples were incorporated into the sample queue to monitor and assess the stability and reliability of the experimental data generated by the system.

 doi:10.20944/preprints202411.1977.v1



Q-TOF mass spectrometry conditions: Analytes were detected using electrospray ionization (ESI) in both positive and negative ion modes. The samples were separated by ultra-high-performance liquid chromatography (UHPLC) and analyzed with a triple TOF 5600 mass spectrometer (Q-TOF, AB SCIEX, USA). The ESI source conditions were optimized as follows: ion source gas 1 (Gas1) set to 60, ion source gas 2 (Gas2) set to 60, curtain gas (CUR) set to 30, source temperature at 600 °C, and IonSpray Voltage Floating (ISVF) at ±5500 V. The TOF MS scan m/z range was 60-1000 Da, while the product ion scan m/z range was 25-1000 Da. The TOF MS scan accumulation time was 0.20 s/spectrum, and the product ion scan accumulation time was 0.05 s/spectrum. The product ion scan was conducted using information-dependent acquisition (IDA) with high sensitivity mode selected. The declustering potential (DP) was set to ±60 V for both positive and negative modes, and the collision energy was set to 35 ± 15 eV. The IDA parameters included the exclusion of isotopes within 4 Da and the monitoring of 6 candidate ions per cycle. The raw MS data (wiff. scan files) were converted to MzXML files using ProteoWizard MSConvert and processed with XCMS for feature detection, retention time correction, and alignment. Metabolites were identified based on precision mass (<25 ppm) and MS/MS data that matched the standard database. For the data extracted by XCMS, only variables with more than 50% non-zero measurement values were retained in at least one group. Pattern recognition was performed using SIMCA-P14.1 software (Umetrics, Umea, Sweden).

After Pareto scaling preprocessing, multidimensional statistical analyses were conducted, including unsupervised principal component analysis (PCA), supervised partial least squares discriminant analysis (PLS-DA), and orthogonal partial least squares discriminant analysis (OPLS-DA). Cross-validation and response permutation were employed for leave-one-out and re-validation to assess the robustness of the model. Significantly different metabolites were identified based on a combination of a statistically significant threshold for variable influence on projection values (VIP) derived from the PLS-DA model and the results of a two-tailed Student's t-test on the raw data. Metabolites with VIP values greater than 1.0 and *P*-values less than 0.1 were deemed significant. Additionally, commercial databases, including KEGG (http://www.genome.jp/kegg/) and MetaboAnalyst (http://www.metaboanalyst.ca/), were utilized to explore metabolite pathways.

## 3. Results

### *3.1. Daily Changes in Greenhouse Environmental Factors*

The diurnal variation of temperature, relative humidity, $CO_2$ concentration, and light intensity in the greenhouse is illustrated in Figure 1. The FC and FT2 treatments reached a maximum temperature of 36 °C at 13:00, while FT1 and FT3 exhibited a similar temperature trend, peaking at 46.3 °C at 12:30 (Figure 1A). No significant differences in $CO_2$ concentration were observed between FC and FT1 treatments. Over time, the $CO_2$ concentration in the greenhouse gradually decreased, reaching its lowest values of 286.77 μmol/mol and 264.96 μmol/mol at 12:00 a.m., respectively. The $CO_2$ concentrations in the FT2 and FT3 treatment groups reached the target level of 1200 μmol/mol 1.5 hours after the experiment commenced, which was significantly different from the concentrations in the FC and FT1 treatments ($P < 0.05$), and this concentration was maintained throughout the experiment. Following the initiation of ventilation at the end of the experiment, the $CO_2$ concentration in the experimental plot decreased rapidly. Subsequently, it stabilized, aligning with $CO_2$ concentrations in FC and FT1 treatments (Figure 1C). The treatments did not have significant differences in relative humidity or light intensity (Figures 1B,D). Overall, the greenhouse conditions for temperature, relative humidity, $CO_2$ concentration, and light intensity met the experimental design requirements throughout the study.

 doi:10.20944/preprints202411.1977.v1



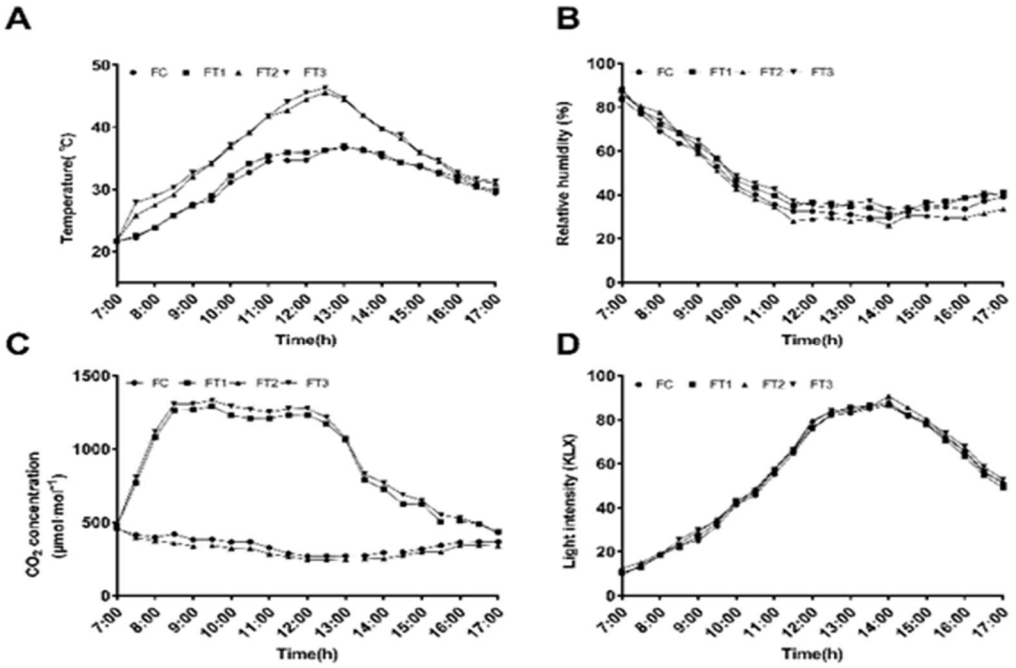


**Figure 1.** Diurnal variation of environmental factors in the greenhouse. (A) Temperature (B) Relative humidity(C) $CO_2$ concentration(D)Light intensity.

*3.2. Effects of Elevated $CO_2$ and High Temperature Stress on Yield and Quality of Cucumber Fruit the Greenhouse*

Cucumbers exhibit different growth centers at various stages of their growth and development. The transition of the growth center to the fruit marks the primary period of yield formation. Measuring the quality of fruit and vegetable products is essential to assess the value characteristics and ensure consumers' health and safety. Figure 2 illustrates that elevated levels of $CO_2$ increased the length (Figure 2A), diameter (Figure 2B), ascorbic acid content (Figure 2C) and soluble sugar content (Figure 2E) of cucumber fruit in both normal and high temperature environments. According to the environmental requirements for the safety, quality, and production of pollutant-free vegetables (GB18407.1-2001), the nitrate content of pollution-free vegetables, in terms of $NaNO_3$, must not exceed 4 mg/kg. The nitrate content of the cucumber fruits subjected to each treatment was consistent with national standards. The nitrate contents of FT3 were significantly lower than those of FC (Figure 2D). The high temperature of 1200±20 μmol/mol $CO_2$(FT3)did not significantly affect the soluble sugar and starch content of cucumber fruit; however, it did result in a substantial increase in the ascorbic acid content, measuring 20.04 ± 0.89 μg/ml.

 doi:10.20944/preprints202411.1977.v1



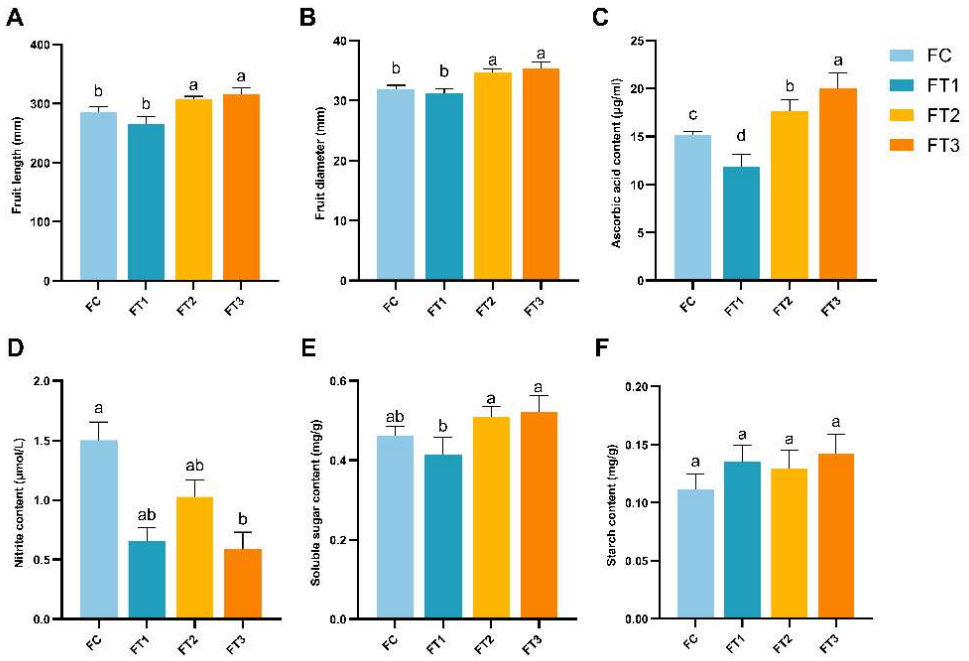


**Figure 2.** Effects of elevated $CO_2$ and high temperature stress on cucumber fruits' length, diameter, and quality. (A) Fruit length (B) Fruit diameter(C) Ascorbic acid content(D) Nitrite content(E) Soluble sugar content. Different lowercase letters were statistically different at the $P < 0.05$ level.

As shown in Table 1, a high temperature of 1200±20 μmol/mol $CO_2$(FT3) improved the number of individual cucumber fruits and increased the total by 14.7% compared to a normal temperature of 1200±20 μmol/mol $CO_2$(FT2). The combination of elevated temperature and $CO_2$ concentration significantly enhanced the number of cucumbers per plant, the weight of each cucumber, and the yield per plant, ultimately resulting in the highest harvest volume within the same picking cycle (35 days).

**Table 1.** Effects of elevated $CO_2$ and high temperature stress on cucumber yield parameter.

| Treatments | Fruit number per plant | Single fruit weight(g) | Yield per plant(g) | Total number of fruits | Total fruit weight(g) |
|---|---|---|---|---|---|
| FC | 4.46±0.02c | 238.29±0.57c | 1281.77±6.06c | 162±0.03c | 46108.74±0.02c |
| FT1 | 3.46±0.09d | 206.93±5.04d | 687.42±0.34d | 121±0.95d | 24712.16±3.61d |
| FT2 | 5.22±0.06b | 284.63±1.01b | 1474.12±6.36b | 185±0.08b | 53033.26±4.06b |
| FT3 | 6.70±0.11a | 291.2±3.33a | 1802.2±0.39a | 217±0.06a | 64844.33±7.36a |

Different lowercase letters were statistically different at the $P < 0.05$ level.

*3.3. Metabolite Profiling and Multivariate Statistical Analysis*

Positive and negative total-ion chromatograms from UHPLC-Q-TOF MS of cucumber fruit metabolomics QC samples were compared to assess spectral overlap. For instance, Figures 3A and 3B illustrate that each chromatographic peak's response intensity and retention time overlapped, with negligible variation due to instrument error during the analysis. XCMS software was utilized to extract ion peaks of metabolites, resulting in the identification of 2505 positive ion peaks and 3136 negative ion peaks. Notably, 79 and 78 significantly different metabolites were identified in the positive and negative modes, respectively. Peaks extracted from all test and QC samples were subjected to PCA analysis following Pareto scaling. The PCA model, validated through 7-fold cross-validation, is presented in Figures 3C and 3D. As depicted, the QC samples are clustered in positive

 doi:10.20944/preprints202411.1977.v1



and negative ion modes, indicating good test repeatability and high data quality. In positive ion mode, the FC group and FT2 group were clustered together. At the same time, FT1 and FT3 formed another cluster, suggesting that temperature has a more pronounced effect on the metabolites of cucumber fruit. In negative ion mode, the metabolomics data of cucumber fruit samples exhibited significant separation under different temperature and $CO_2$ conditions. Notably, FT3 was significantly distinct from the other three groups, indicating that the high temperature combined with elevated $CO_2$ (1200 ± 20 μmol/mol) in FT3 led to significant differences in metabolite profiles compared to the other groups (Figure 3D). In summary, the stability of the test instrument analysis system is commendable, and the test data is both stable and reliable. The metabolic profiles obtained in this experiment effectively reflect the biological differences among cucumber fruit samples subjected to various treatments.

The model parameters were derived from partial least squares discriminant analysis (PLS-DA) and orthogonal partial least squares discriminant analysis (OPLS-DA) of the differential metabolites between groups, as presented in Table 2. The closer the values of $R^2$ and $Q^2$ are to 1, the more stable and reliable the model becomes. In this experiment, the PLS-DA model was constructed using positive and negative ion modes data, achieving $R^2$ and $Q^2$ values $\geqslant$ 0.5, indicating that the model is stable and reliable. For the OPLS-DA model, the parameters were $R^2Y > 0.9$, $Q^2 > 0.5$, and a permutation intercept of $Q^2_{intercept} < 0$ (see Supplementary Figure S1). The OPLS-DA model established from this experiment's positive and negative ion-mode data is thus deemed reasonable, stable, and reliable.

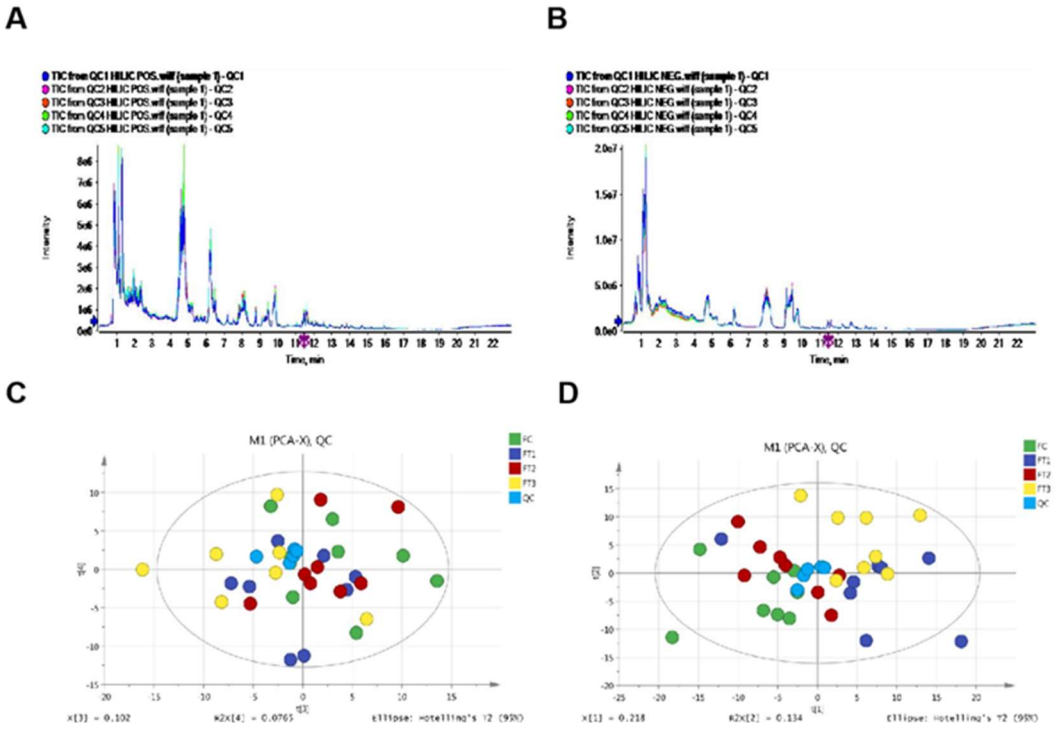


**Figure 3.** (A) Positive ion model TIC spectral overlap of QC samples (B) Negative ion model TIC spectral overlap of QC samples (C) PCA score diagram under positive ion pattern (D) PCA score diagram under negative ion pattern.

**Table 2.** Metabonomics of cucumber fruits PLS-DA and OPLS-DA model parameters.

| Treatments | PLS-DA | | | | OPLS-DA | | | |
|---|---|---|---|---|---|---|---|---|
| | POS Models | | NEG Models | | POS Models | | NEG Models | |
| | $R^2Y$ | $Q^2$ | $R^2Y$ | $Q^2$ | $R^2Y$ | $Q^2$ | $R^2Y$ | $Q^2$ |
| FT1-FC | 0.98 | 0.765 | 0.997 | 0.787 | 0.98 | 0.7 | 0.979 | 0.633 |
| FT2-FC | 0.911 | 0.587 | 0.941 | 0.21 | 0.957 | 0.689 | 0.941 | 0.272 |

 doi:10.20944/preprints202411.1977.v1



| | | | | | | | | |
|---|---|---|---|---|---|---|---|---|
| FT3-FT1 | 0.998 | 0.798 | 0.996 | 0.82 | 0.95 | 0.571 | 0.985 | 0.721 |
| FT3-FT2 | 0.992 | 0.903 | 0.988 | 0.776 | 1 | 0.765 | 1 | 0.85 |

### *3.4. Comparison of the Number of Differential Metabolites in Cucumber Fruit Under Elevated $CO_2$ and High-Temperature Stress*

Utilizing univariate analysis, the significance of metabolite changes between the two samples can be visually represented, facilitating the selection of potential marker metabolites based on the screening criteria of fold change (FC) > 2.0 and *P*-value < 0.05, as identified through univariate statistical analysis. The volcanic maps of differential metabolites in cucumber fruits under both positive and negative ion modes are illustrated in Figures 4 and 5. These figures depict the distribution of metabolites, with red dots representing a higher concentration of metabolites with minor fold differences. In contrast, blue dots are more dispersed, indicating larger fold differences. The blue dots in the figure correspond to metabolites with FC > 2.0 and *P*-value < 0.05, which are the differential metabolites identified through univariate statistical analysis.

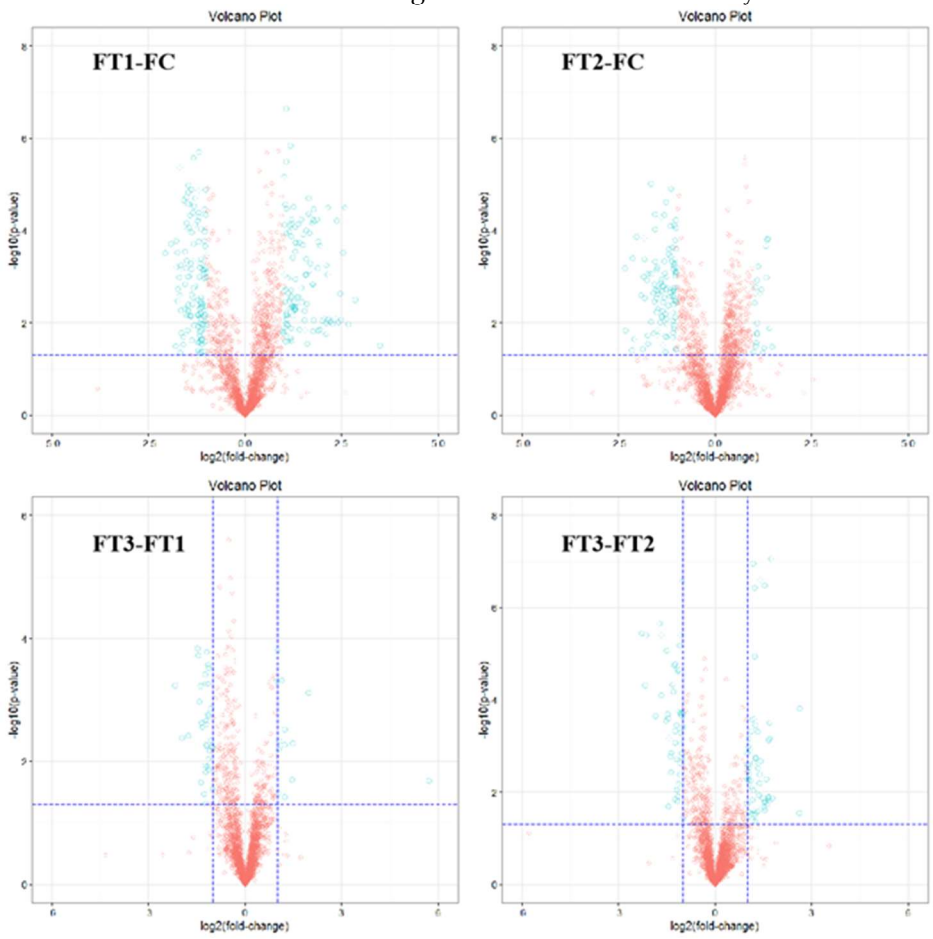


**Figure 4.** Volcanic diagram of differential metabolites in cucumber fruits in positive ion mode.

 doi:10.20944/preprints202411.1977.v1



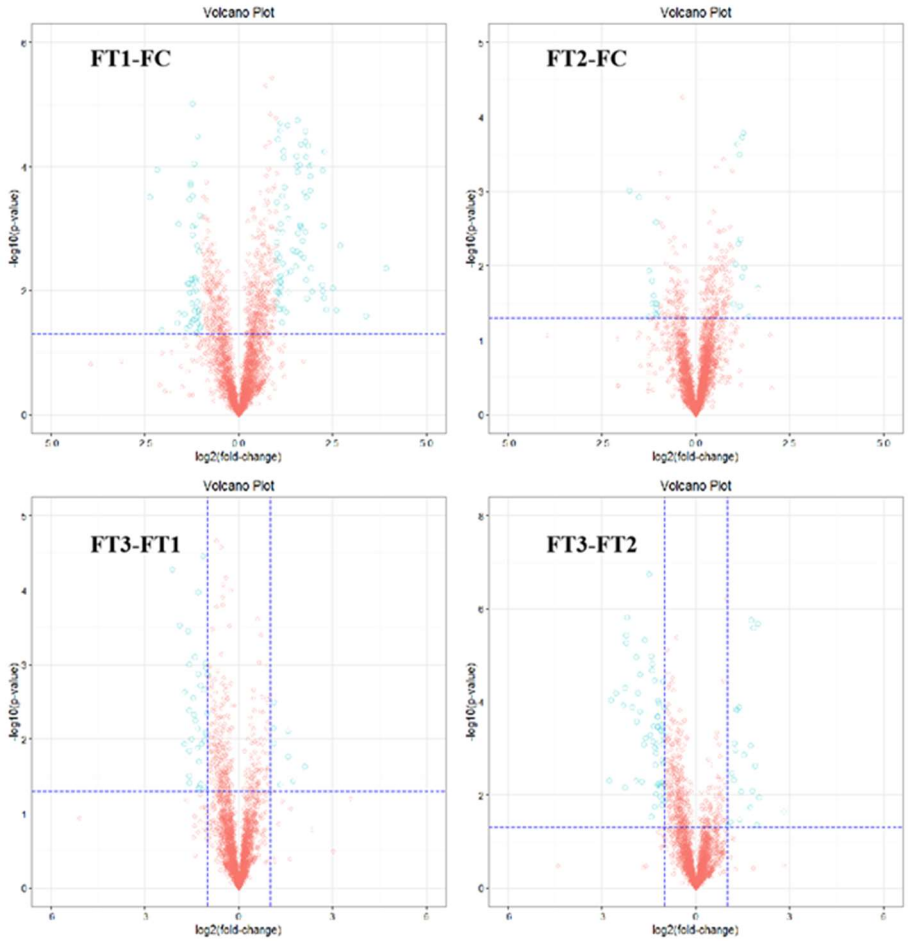


**Figure 5.** Volcanic diagram of differential metabolites in cucumber fruits in negative ion mode.

As shown in Figure 6, in the positive ion mode, the FT1-FC group exhibited 20 upregulated metabolites and 11 downregulated metabolites. The FT2-FC group showed 9 upregulated and 6 downregulated metabolites, while the FT3-FT1 group had 6 upregulated and 7 downregulated metabolites. In the FT3-FT2 comparison, there were 13 upregulated and 7 downregulated metabolites. The FT1-FC group revealed 17 upregulated and 10 downregulated metabolites in the negative ion mode. The FT2-FC group had 10 upregulated and 9 downregulated metabolites; the FT3-FT1 group displayed 6 upregulated and 8 downregulated metabolites, and the FT3-FT2 group showed 8 upregulated and 10 downregulated metabolites. Overall, in both positive and negative ion modes, the FT1-FC group (high temperature of 400±20 ppm $CO_2$ - normal temperature of 400±20 ppm $CO_2$) presented 37 upregulated and 21 downregulated metabolites. The FT2-FC group (normal temperature of 1200±20 ppm $CO_2$ + normal temperature of 400±20 ppm $CO_2$) exhibited 19 upregulated and 15 downregulated metabolites. In the FT3-FT1 group (high temperature of 1200±20 ppm $CO_2$ + high temperature of 400±20 ppm $CO_2$), there were 12 upregulated and 15 downregulated metabolites. The FT3-FT2 group (high temperature of 1200±20 ppm $CO_2$ + normal temperature of 1200±20 ppm $CO_2$) showed 21 upregulated and 17 downregulated metabolites. Notably, the effect of temperature on the metabolites of cucumber fruit was more pronounced.

 doi:10.20944/preprints202411.1977.v1



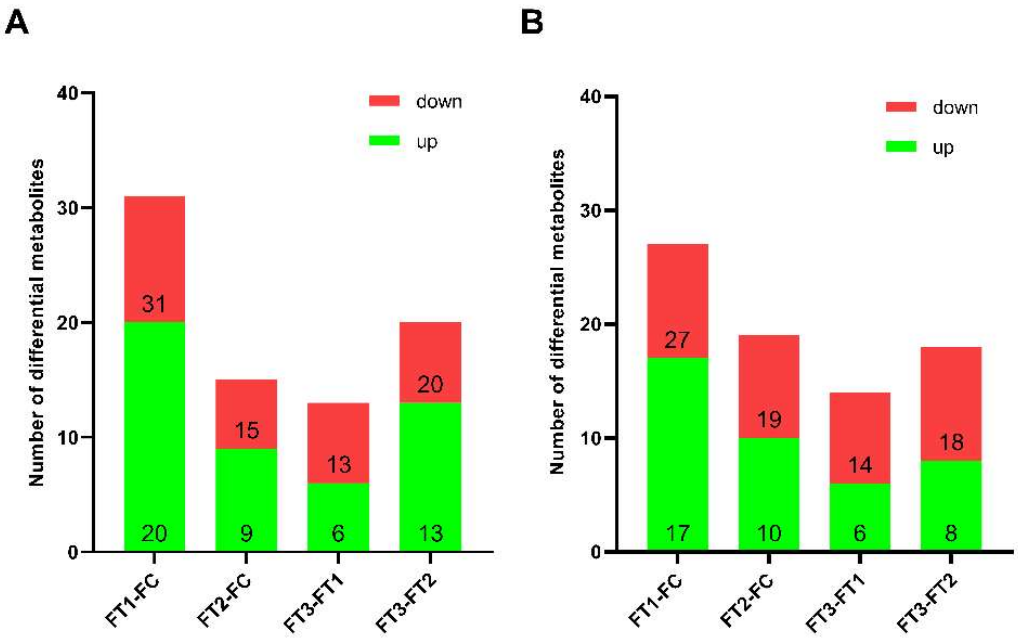


**Figure 6.** Comparative analysis of the number of up-regulated and down-regulated metabolites in cucumber fruits between different treatments. (A) Positive ion model (B) Negative ion model.

*3.5. Significant Differences in Metabolites of Cucumber Fruit under Elevated $CO_2$ and High-Temperature Stress Conditions.*

To identify differential metabolites, we selected those with a multidimensional statistical analysis VIP > 1 and a univariate statistical analysis *P*-value of 1, with 0.05 < *P*-value < 0.1. As shown in Tables 3 and 4, in both positive and negative ion modes, the FT1-FC group exhibited significant increases in sugar and amino acid metabolites, including glycerophosphocholine, adenosine, sucrose, isomaltose, mannose, arginine, L-citrulline, and L-isoleucine, in cucumber fruits treated at normal temperature. The FT2-FC group showed up-regulation of differential metabolites such as D-mannose and glycerophosphate. In the FT3-FT1 comparison group, L-glutamic acid, adenosine, and phosphorylcholine metabolites were up-regulated. Similarly, in the FT3-FT2 comparison group, metabolites, including L-glutamic acid, adenine, sucrose, and D-mannose, were significantly up-regulated. In the high-temperature treatment comparison group, lipids, sugars, and nucleotides were the predominant up-regulated metabolites. In the negative ion mode, sugars and amino acids emerged as the most up-regulated metabolites. Furthermore, organic acid, sugar, and amino acid metabolites collectively regulated the differential changes observed in the fruits, responding to high-temperature stress in cucumber fruits.

**Table 3.** Results of screening differential metabolites among treatments in cucumber fruits under the positive-ion model.

 doi:10.20944/preprints202411.1977.v1



| Treatment | Adduct | Description | VIP | Fold change | *P*-value | m/z |
|---|---|---|---|---|---|---|
| | (M+H)+ | N6-Acetyl-L-lysine | 1.1042 | 2.106173432 | 2.27E-07 | 189.1229777 |
| | (M+NH4)+ | Stachyose | 2.10089 | 3.430945331 | 3.46792E-05 | 684.2540647 |
| | (M+H)+ | Isoleucyl-Leucine | 1.1676 | 0.495955584 | 4.59299E-05 | 245.1857351 |
| | (M+NH4)+ | Galactinol | 1.90038 | 3.258320781 | 5.22239E-05 | 360.1495983 |
| | (M+H)+ | DL-2-Aminoadipic acid | 2.57705 | 2.251552694 | 7.77606E-05 | 162.0756954 |
| | (M+H)+ | Adenosine | 4.48684 | 3.7050105 | 0.000173939 | 268.1036817 |
| | (M+H-H2O)+ | MG(16:0) | 2.33826 | 0.267244704 | 0.000199512 | 313.2734126 |
| | (M+H)+ | Guanosine | 1.08141 | 0.52847139 | 0.00056931 | 284.0984148 |
| | (M+H)+ | L-Glutamate | 2.53344 | 2.979179578 | 0.00090144 | 148.060162 |
| | M+ | Glycerophosphocholine | 4.17697 | 2.015781719 | 0.00091951 | 258.1100798 |
| | (M+H)+ | Uracil | 1.97467 | 0.660483819 | 0.00200466 | 113.0337225 |
| | (M+H)+ | Uridine 5'-monophosphate (UMP) | 2.22288 | 1.964642529 | 0.002301128 | 325.043038 |
| | (M+H)+ | L-Histidine | 1.38928 | 5.516521084 | 0.002324441 | 156.0761414 |
| | (M+H)+ | L-Pyroglutamic acid | 1.46197 | 1.783756434 | 0.002797668 | 130.0493144 |
| | (M+H)+ | Leucyl-Valine | 1.18864 | 0.456223529 | 0.00285914 | 231.1697036 |
| FT1-FC | (M+H)+ | Adenosine monophosphate (AMP) | 2.04171 | 7.182241423 | 0.00321324 | 348.0699186 |
| | (M+H)+ | Dulcitol | 1.49033 | 2.490899932 | 0.003893796 | 183.0857094 |
| | (M+H)+ | L-Phenylalanine | 1.56216 | 1.449125698 | 0.005090748 | 166.0857143 |
| | (M+H)+ | LysoPC(18:1(9Z)) | 1.52475 | 0.364249447 | 0.005665312 | 522.3506739 |
| | (M+H)+ | LysoPC(16:0) | 1.3079 | 0.454880625 | 0.00631801 | 496.3382226 |
| | (M+H)+ | Uridine | 2.642 | 0.680180759 | 0.00663179 | 245.0760895 |
| | (M+H)+ | Adenine | 4.92408 | 0.643645209 | 0.007278359 | 136.0608864 |
| | (M+NH4)+ | myo-Inositol | 1.3025 | 1.334571795 | 0.007386832 | 198.096974 |
| | (M+NH4)+ | Sucrose | 5.01279 | 4.828276583 | 0.01042811 | 360.1494567 |
| | (M+H)+ | LysoPE(16:0/0:0) | 1.37852 | 0.36084323 | 0.014736436 | 454.2910991 |
| | (M+NH4)+ | Isomaltose | 2.17888 | 1.949730777 | 0.021699484 | 360.1497688 |
| | (M+NH4)+ | D-Mannose | 3.31788 | 1.218994235 | 0.023118102 | 198.0970991 |
| | (M+H)+ | D-Pipecolic acid | 3.36975 | 1.444725373 | 0.05282959 | 130.0855724 |
| | (M+H)+ | L-Arginine | 1.83065 | 1.539305717 | 0.071148604 | 175.1187363 |
| | (M+H)+ | L-Citrulline | 3.21868 | 0.52192839 | 0.074571343 | 176.1028292 |
| | (M+H)+ | L-Isoleucine | 1.07822 | 1.284940343 | 0.083495926 | 132.1011794 |
| | (M+H)+ | Uridine 5'-monophosphate (UMP) | 2.32809 | 1.809470709 | 2.30648E-05 | 325.043038 |
| | (M+H)+ | Adenosine | 3.40403 | 2.479642634 | 0.000224186 | 268.1036817 |
| | (M+H-H2O)+ | MG(16:0) | 2.25847 | 0.390912457 | 0.00158598 | 313.2734126 |
| | (M+H)+ | L-Glutamate | 1.76742 | 1.799871016 | 0.00280578 | 148.060162 |
| | (M+H)+ | LysoPC(18:1(9Z)) | 1.45425 | 0.420733502 | 0.008301088 | 522.3506739 |
| | (M+H)+ | DL-2-Aminoadipic acid | 1.57208 | 1.504933045 | 0.008835885 | 162.0756954 |
| | (M+NH4)+ | D-Mannose | 4.07313 | 1.17072483 | 0.017972586 | 198.0970991 |
| FT2-FC | (M+H)+ | LysoPE(16:0/0:0) | 1.35687 | 0.412319275 | 0.019955166 | 454.2910991 |
| | (M+H)+ | LysoPC(16:0) | 1.84559 | 0.423830619 | 0.020233127 | 496.3385749 |
| | (M+NH4)+ | myo-Inositol | 1.40704 | 1.259170086 | 0.025954155 | 198.096974 |
| | M+ | Glycerophosphocholine | 2.54532 | 1.383717449 | 0.028200106 | 258.1100798 |
| | (M+NH4)+ | Stachyose | 1.30302 | 1.897151257 | 0.033226899 | 684.2540647 |
| | (M+NH4)+ | Galactinol | 1.08617 | 1.704275817 | 0.041890007 | 360.1495983 |
| | (M+H-H2O)+ | Sucrose | 1.43032 | 1.525572677 | 0.069972456 | 325.1125745 |
| | (M+H)+ | S-Methyl-5'-thioadenosine | 2.90396 | 0.732635606 | 0.08277411 | 298.0968052 |
| | (M+H)+ | L-Glutamate | 4.20574 | 2.004753618 | 0.000165263 | 148.060162 |
| | (M+H)+ | N6-Acetyl-L-lysine | 1.05864 | 0.65310727 | 0.000180881 | 189.1229777 |
| | (M+H)+ | Uridine 5'-diphosphate (UDP) | 1.25396 | 3.931667725 | 0.000779497 | 405.0087465 |
| | (M+H)+ | Adenosine | 5.29102 | 1.601485812 | 0.021435996 | 268.1036817 |
| | (M+H)+ | L-Phenylalanine | 2.2571 | 0.657415721 | 0.028471787 | 166.0857143 |
| | (M+Na)+ | LysoPC(16:0) | 1.57464 | 1.831620564 | 0.034998726 | 518.3223979 |
| FT3-FT1 | (M+H-H2O)+ | Tyramine | 1.35054 | 0.669090063 | 0.036569592 | 120.0800541 |
| | (M+H)+ | Phosphorylcholine | 4.2875 | 0.530379573 | 0.055143529 | 184.0728675 |
| | (M+H)+ | Glutathione disulfide | 1.29319 | 1.459068312 | 0.060741402 | 613.1579239 |
| | (M+H)+ | L-Histidine | 1.43458 | 0.508182362 | 0.071838225 | 156.0761414 |
| | (M+CH3COO+2H) | (S)-(-)-Citronellic acid | 1.25486 | 0.713691538 | 0.079271811 | 231.1587002 |
| | (M+H)+ | Dulcitol | 1.21446 | 0.664957482 | 0.084053051 | 183.0857094 |
| | (M+NH4)+ | Stachyose | 1.47216 | 1.285834336 | 0.090587542 | 684.2540647 |
| | (M+H)+ | L-Glutamate | 4.54822 | 3.318305025 | 8.75235E-08 | 148.060162 |
| | (M+H)+ | L-Pyroglutamic acid | 2.78278 | 2.270096754 | 1.13216E-07 | 130.0493144 |
| | (M+H)+ | Isoleucyl-Leucine | 1.14926 | 0.426060216 | 1.70538E-05 | 245.1857351 |
| | (M+H)+ | Adenine | 6.35041 | 0.536454007 | 0.000107524 | 136.0608864 |
| | (M+H)+ | Uridine 5'-diphosphate (UDP) | 1.31965 | 6.195503464 | 0.000157421 | 405.0087465 |
| | (M+NH4)+ | Stachyose | 2.4361 | 2.325395667 | 0.000259314 | 684.2540647 |
| | (M+H)+ | Adenosine monophosphate (AMP) | 2.4176 | 3.224507881 | 0.000319113 | 348.0699186 |
| | (M+H)+ | Adenosine | 5.80057 | 2.392893907 | 0.00035694 | 268.1036817 |
| | (M+H)+ | Phosphorylcholine | 4.02879 | 0.506034609 | 0.002934398 | 184.0728675 |
| FT3-FT2 | (M+H)+ | Pyridoxal (Vitamin B6) | 1.34229 | 0.52359965 | 0.003142514 | 168.0648829 |
| | (M+NH4)+ | Galactinol | 1.80857 | 2.04767815 | 0.003724976 | 360.1495983 |
| | (M+H)+ | L-Citrulline | 2.33731 | 0.521157833 | 0.005522411 | 176.1025882 |
| | (M+NH4)+ | Sucrose | 5.73273 | 3.173523813 | 0.015467808 | 360.1494567 |
| | (M+NH4)+ | myo-Inositol | 1.25201 | 2.721135173 | 0.021130467 | 198.0966671 |
| | (M+H)+ | L-Aspartate | 1.16444 | 1.392992743 | 0.042748309 | 134.0443811 |
| | (M+H-H2O)+ | MG(16:0) | 1.08828 | 0.611113055 | 0.049775757 | 313.2732432 |
| | (M+NH4)+ | D-Mannose | 4.83972 | 1.130577842 | 0.062991447 | 198.097091 |
| | (M+H)+ | S-Methyl-5'-thioadenosine | 1.98845 | 1.342751917 | 0.079937188 | 298.0966306 |
| | (M+H)+ | Erucamide | 1.00923 | 1.706158843 | 0.087463144 | 338.3410313 |
| | (M+H)+ | Uracil | 1.31395 | 0.804266602 | 0.095577127 | 113.0337225 |

**Table 4.** Results of screening differential metabolites among treatments in cucumber fruits under negative ion mode.

 doi:10.20944/preprints202411.1977.v1



| Treatment | Adduct | Description | VIP | Fold change | p-value | m/z |
|---|---|---|---|---|---|---|
| | (M-H)- | Galactinol | 2.77527 | 3.137884288 | 4.4603E-05 | 341.1094001 |
| | (M-H2O-H)- | alpha-D-Galactose 1-phosphate | 1.46665 | 0.441852624 | 9.20693E-05 | 241.0123061 |
| | (M-H)- | Adenosine | 1.37392 | 3.846112898 | 9.62984E-05 | 266.0895495 |
| | (M-H)- | Stachyose | 1.50325 | 2.94439035 | 0.000100591 | 665.2159064 |
| | (M-H)- | DL-2-Aminoadipic acid | 2.14587 | 2.334897767 | 0.000216539 | 160.0615993 |
| | (M-H)- | Glyceric acid | 4.29502 | 1.387719768 | 0.001442725 | 105.0189954 |
| | (M-H)- | Adenine | 5.42611 | 0.554640098 | 0.001466814 | 134.0470177 |
| | (M-H)- | Adenosine monophosphate (AMP) | 1.39543 | 6.537282039 | 0.001876124 | 346.0558902 |
| | (M-H)- | Xylitol | 1.41849 | 1.451859513 | 0.002526913 | 151.06112 |
| | (M-H)- | Guanosine | 1.04731 | 0.553212713 | 0.002584757 | 282.0842734 |
| | (M-H)- | L-Glutamate | 2.66584 | 3.335986525 | 0.002997717 | 146.0459671 |
| | (M-H)- | Uridine 5'-monophosphate (UMP) | 2.33096 | 1.972748206 | 0.003122165 | 323.0290515 |
| | (M-H)- | D-Mannose | 8.68215 | 1.24275597 | 0.007343744 | 179.0564815 |
| FT1-FC | (M+CH3COO)- | Uridine | 2.2763 | 0.596198059 | 0.007605074 | 303.0834516 |
| | (M+CH3COO)- | D-Fructose | 8.27271 | 1.293548526 | 0.008865282 | 239.0777658 |
| | (M-H)- | DL-lactate | 1.67437 | 1.197964422 | 0.011350669 | 89.02393999 |
| | (M-H)- | Heptadecanoic acid | 1.00866 | 0.77439784 | 0.01485783 | 269.2481757 |
| | (M-H)- | Uracil | 2.21839 | 0.422065826 | 0.015973334 | 111.0194812 |
| | (M-H)- | L-Threonate | 1.1167 | 0.668055502 | 0.020038333 | 135.0297033 |
| | (M-H)- | Pentadecanoic Acid | 1.95144 | 0.632001813 | 0.021000835 | 241.2169708 |
| | (M-H)- | Sucrose | 2.13426 | 1.897067552 | 0.023953897 | 341.1091902 |
| | (M-H)- | myo-Inositol | 2.6195 | 1.211907563 | 0.03432838 | 179.0566938 |
| | (M-H)- | Alpha-D-Glucose | 2.20517 | 1.253765515 | 0.040685725 | 179.0563233 |
| | (M-H)- | Dihydroxyacetone | 1.4467 | 1.155668972 | 0.067132119 | 89.02385541 |
| | (M-H)- | Succinate | 1.84195 | 0.743181741 | 0.075366429 | 117.0193115 |
| | (M-H)- | L-Citrulline | 2.40279 | 0.483989036 | 0.083647655 | 174.0886716 |
| | (M-H)- | L-Pipecolic acid | 1.55107 | 1.393968143 | 0.097476798 | 128.0713519 |
| | (M-H)- | Adenosine | 1.3809 | 2.401842906 | 0.000165087 | 266.0895495 |
| | (M-H)- | Uridine 5'-monophosphate (UMP) | 2.77846 | 1.668489359 | 0.000373825 | 323.0290515 |
| | (M-H2O-H)- | alpha-D-Galactose 1-phosphate | 1.53692 | 0.669046883 | 0.004191403 | 241.0123061 |
| | (M-H2O-H)- | Dihydroxyacetone | 2.64556 | 0.69223488 | 0.010859544 | 71.0133543 |
| | (M-H)- | D-Mannose | 4.00873 | 1.106442071 | 0.014607796 | 179.0564903 |
| | (M-H)- | Pentadecanoic Acid | 2.57158 | 0.641181177 | 0.015992475 | 241.2169708 |
| | (M-H)- | L-Glutamate | 1.78951 | 1.637605439 | 0.020678644 | 146.0459671 |
| | (M-H)- | Allantoin | 1.03388 | 0.70012673 | 0.023063641 | 157.0364845 |
| | (M-H)- | DL-2-Aminoadipic acid | 1.41451 | 1.487326126 | 0.031607012 | 160.0615993 |
| FT2-FC | (M-H)- | Citramalic acid | 1.08133 | 1.386067936 | 0.037988482 | 147.0296172 |
| | (M-H)- | Vanillin | 4.19215 | 1.384558698 | 0.060790967 | 151.0399781 |
| | (M+CH3COO)- | D-Fructose | 7.8993 | 1.159578626 | 0.062552147 | 239.0777658 |
| | (M-H)- | Alpha-D-Glucose | 12.3963 | 1.171955636 | 0.071036447 | 179.0564446 |
| | (M-H)- | L-Citrulline | 3.74037 | 0.476035223 | 0.071310415 | 174.0886716 |
| | (M-H)- | L-Pyroglutamic acid | 2.04925 | 0.727312883 | 0.080174244 | 128.0348987 |
| | (M-H)- | L-Glutamine | 7.45031 | 0.785930958 | 0.084280094 | 145.062161 |
| | (M-H)- | Dihydrothymine | 2.26349 | 0.787664968 | 0.085279151 | 127.0510727 |
| | (M-H)- | Dodecanoic acid | 1.90232 | 0.730163708 | 0.086315991 | 199.1702574 |
| | (M-H)- | Galactinol | 1.32481 | 1.479842859 | 0.089838008 | 341.1094001 |
| | (M-H)- | L-Glutamate | 3.61653 | 1.959665343 | 0.002632325 | 146.0459671 |
| | (M-H)- | Glyceric acid | 4.24449 | 0.784807483 | 0.00283771 | 105.0189954 |
| | (M-H)- | Xylitol | 1.09041 | 0.714046375 | 0.003308492 | 151.0610404 |
| | (M-H)- | Myristic acid | 9.36492 | 0.532774245 | 0.006392923 | 227.2018088 |
| | (M-H)- | Pentadecanoic Acid | 1.92914 | 0.580205097 | 0.011736974 | 241.2169708 |
| | (M-H2O-H)- | alpha-D-Galactose 1-phosphate | 1.06241 | 0.442767335 | 0.011761039 | 241.0123061 |
| FT3-FT1 | (M-H)- | all cis-(6,9,12)-Linolenic acid | 19.7514 | 2.050396663 | 0.01495541 | 277.2174491 |
| | (M-H)- | L-Asparagine | 1.06012 | 0.688255233 | 0.017708502 | 131.0459105 |
| | (M-H)- | Adenosine | 1.1566 | 1.524046784 | 0.025926068 | 266.0895495 |
| | (M-H)- | L-Pyroglutamic acid | 1.95893 | 0.650425631 | 0.026479617 | 128.0348987 |
| | (2M-H)- | alpha-Linolenic acid | 6.63087 | 3.341824389 | 0.037203389 | 555.4407713 |
| | (M-H)- | L-Phenylalanine | 1.21334 | 0.65522841 | 0.039534218 | 164.071433 |
| | (M-H)- | Succinate | 1.99799 | 1.356737163 | 0.06584506 | 117.0193115 |
| | (M-H)- | Uracil | 1.57198 | 1.694606499 | 0.066768761 | 111.0194812 |
| FT3-FT2 | (M-H)- | L-Glutamate | 4.47049 | 3.992058784 | 2.12289E-06 | 146.0459671 |
| | (M-H2O-H)- | alpha-D-Galactose 1-phosphate | 1.34402 | 0.292412854 | 2.64736E-05 | 241.0123061 |
| | (M-H)- | Adenine | 5.76247 | 0.487044403 | 3.74277E-05 | 134.0470177 |
| | (M-H)- | Adenosine | 1.57485 | 2.440482672 | 0.00014746 | 266.0895495 |
| | (M-H)- | Stachyose | 1.61666 | 2.345314 | 0.000790485 | 665.2159064 |
| | (M-H)- | Adenosine monophosphate (AMP) | 1.60239 | 3.383421046 | 0.000889008 | 346.0558902 |
| | (M-H)- | Pentadecanoic Acid | 1.66985 | 0.571898687 | 0.00239706 | 241.2169708 |
| | (M-H)- | Galactinol | 2.42145 | 2.206388517 | 0.003507879 | 341.1094001 |
| | (M-H)- | Sucrose | 7.68865 | 3.485124847 | 0.008314919 | 341.1091339 |
| | (M-H)- | D-Ribose | 2.15376 | 0.672464793 | 0.009151401 | 149.0452312 |
| | (M-H)- | LysoPE(16:0/0:0) | 1.31927 | 0.729075753 | 0.023480402 | 452.278056 |
| | (M+CH3COO)- | Uridine | 1.56591 | 0.752610312 | 0.033535592 | 303.0834516 |
| | (2M-H)- | Palmitic acid | 1.20898 | 0.582921901 | 0.043646522 | 511.4718732 |
| | (M-H)- | Maleic acid | 2.56365 | 1.177316096 | 0.059340422 | 115.0034172 |
| | (M-H)- | Myristic acid | 5.2123 | 0.66946221 | 0.074228979 | 227.2018088 |
| | (M-H)- | ketoisocaproic acid | 3.64571 | 0.572488647 | 0.080468735 | 129.0554357 |
| | (M+CH3COO)- | D-Fructose | 5.67541 | 1.08993369 | 0.095477634 | 239.0776264 |
| | (M-H)- | Vanillin | 2.40631 | 0.781198008 | 0.09904225 | 151.0399781 |

### *3.6. Cluster Analysis of Elevated $CO_2$ and High-temperature Stress Conditions of Differential Metabolic Levels in Cucumber Fruit*

 doi:10.20944/preprints202411.1977.v1



Figure 7 illustrates the clustering results of differential metabolites in cucumber fruits cultivated in greenhouses under various combinations of temperature and $CO_2$, analyzed in both positive and negative ion modes. The tree-type heat map indicates that red signifies up-regulation while blue indicates down-regulation. The abscissa represents the samples, the coordinates denote the differential metabolites, and the branch lengths reflect the differences between the samples and the metabolites; longer branches indicate a more significant difference between the two metabolites. Figure 8 presents a Venn diagram of the differential metabolites across different treatments. The non-overlapping sections of the diagram are unique to each group. The labels on the Venn diagram indicate the number of common and unique substances between the various treatment combinations, expressed in quantity and percentage. Additionally, the bar graph displays the total number of substances in each group.

Significant differences were observed in the differential metabolites of cucumber fruits grown in a greenhouse under varying temperatures and $CO_2$ concentrations. In both positive and negative ion modes, 58 differential metabolites were identified under FT1-FC (high temperature of 400±20 ppm $CO_2$ - normal temperature of 400±20 ppm $CO_2$), with 20 metabolites unique to FT1-FC. Significantly different metabolites included guanosine, leucyl-valine, uridine, isomaltose, xylitol, D-mannose, DL-lactate, heptadecanoic acid, L-threonate, sucrose, myo-inositol, and alpha-D-glucose. Under FT2-FC (normal temperature of 1200±20 ppm $CO_2$ + normal temperature of 400±20 ppm $CO_2$), 34 differential metabolites were identified, of which 11 were specific to FT2-FC. Significantly different metabolites included dihydroxyacetone, D-mannose, allantoin, and citric acid. In the FT3-FT1 (high temperature of 1200±20 ppm $CO_2$ + high temperature of 400±20 ppm $CO_2$), 27 differential metabolites were identified, with 9 unique to FT3-FT1. Significant metabolites in this group included tyramine, xylitol, all cis-(6,9,12)-linolenic acid, L-asparagine, alpha-linolenic acid, and L-phenylalanine. Additionally, 38 differential metabolites were identified under FT3-FT2 (high temperature of 1200±20 ppm $CO_2$ + normal temperature of 1200±20 ppm $CO_2$), with 15 unique to FT3-FT2. Significantly different metabolites included pyridoxal (vitamin B6), L-citrulline, myo-inositol, L-aspartate, MG (16:0), sucrose, D-ribose, and palmitic acid. High temperatures induced alterations in the levels of amino acids, sugars, and organic acid metabolites in cucumber fruits. The changes in sugars and differential metabolites of organic acids, resulting from variations in $CO_2$ concentration, were closely linked to the transport of starch and soluble sugars, which are critical for assessing the physiological indices of the fruits.

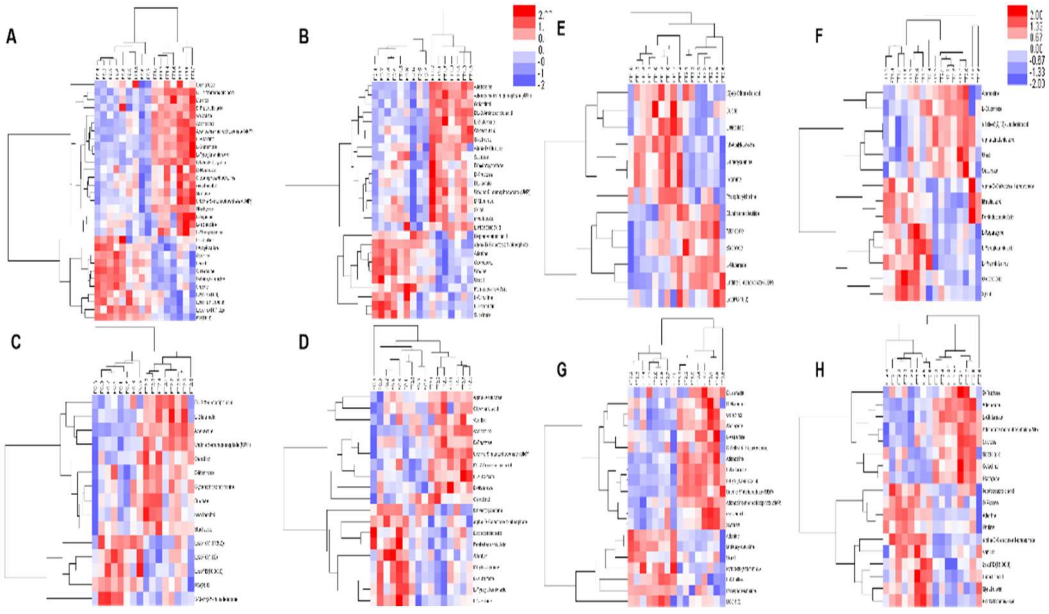


**Figure 7.** Group analysis of differential metabolites (A) FT1-FC, positive ion model (B) FT1-FC, negative ion mode (C) FT2-FC, positive ion model (D) FT2-FC, negative ion mode (E) FT3-FT1, positive ion model (F) FT3-FT1, negative ion mode (G) FT3-FT2, positive ion model (H) FT3-FT2, negative ion mode.

 doi:10.20944/preprints202411.1977.v1



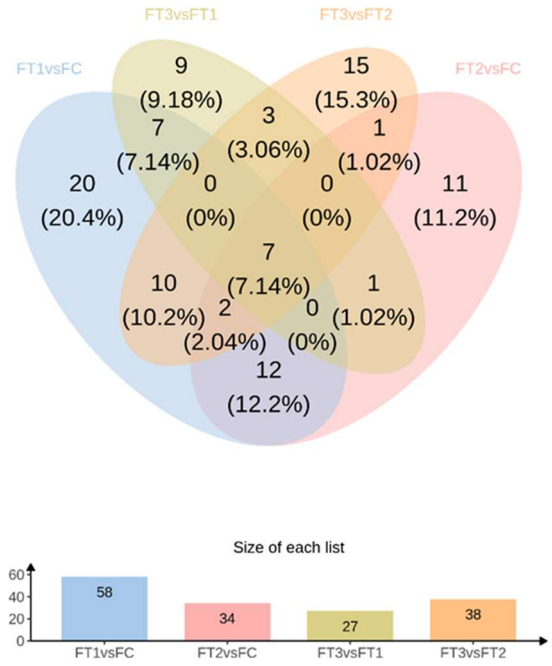


**Figure 8.** Different metabolites between different treatments Venn diagram (Venn) combined histogram.

*3.7. Enrichment Analysis of the KEGG Annotation of Differential Metabolites in Cucumber Fruit*

The enrichment analysis of annotations related to the KEGG pathway for target metabolite sets in greenhouse cucumber fruit was conducted by treating each KEGG pathway as a unit and utilizing all metabolites within each pathway as the background. Fisher's exact test was employed to compare the distribution of each KEGG pathway within the target metabolite set against the overall metabolite set, thus evaluating the significance level of KEGG pathway metabolite enrichment. The x-axis represents the enrichment impact factor, while the y-axis indicates the names of the pathway diagrams. The color of the histogram illustrates the magnitude of the *P*-value. In the analysis of differentially expressed metabolites under FT1-FC, 58 metabolic pathways were identified, of which 14 were significantly enriched. Specifically, 6 differentially expressed metabolites were enriched in the galactose metabolic pathway(map00052),3 in the vitamin B6 metabolism(map00750), and 3 in the arginine biosynthetic pathway(map00220). Enriching differentially expressed metabolites at FT2-FC involved 34 metabolic pathways; 6 differentially expressed metabolites were associated with the galactose metabolic pathway(map00052). In contrast, 3 differentially expressed metabolites were enriched in the arginine metabolic pathway(map00220) and 2 in the glutamate biosynthetic pathway(map00471). The enrichment of differentially expressed metabolites under FT3-FT1 encompassed 47 metabolic pathways, with 15 significantly enriched pathways. Within this context, 3 differentially expressed metabolites were identified in the metabolic pathways of alanine, aspartic acid, and glutamic acid(map00250). Furthermore, 3 differentially expressed metabolites were enriched in the glutathione metabolic pathways(map00480), while another 3 were associated with the glyoxylate and dicarboxylate metabolic pathways(map00630). The analysis of differentially expressed metabolites at FT3-FT2 revealed 43 metabolic pathways, including 14 significantly enriched ones. Notably, 5 differentially expressed metabolites were enriched in the galactose metabolic pathway(map00052), 4 were linked to the zeatin biosynthesis pathway(map00908), 3 were related to arginine biosynthesis(map00220), and 3 were closely associated with pyrimidine metabolism (map00240).

 doi:10.20944/preprints202411.1977.v1



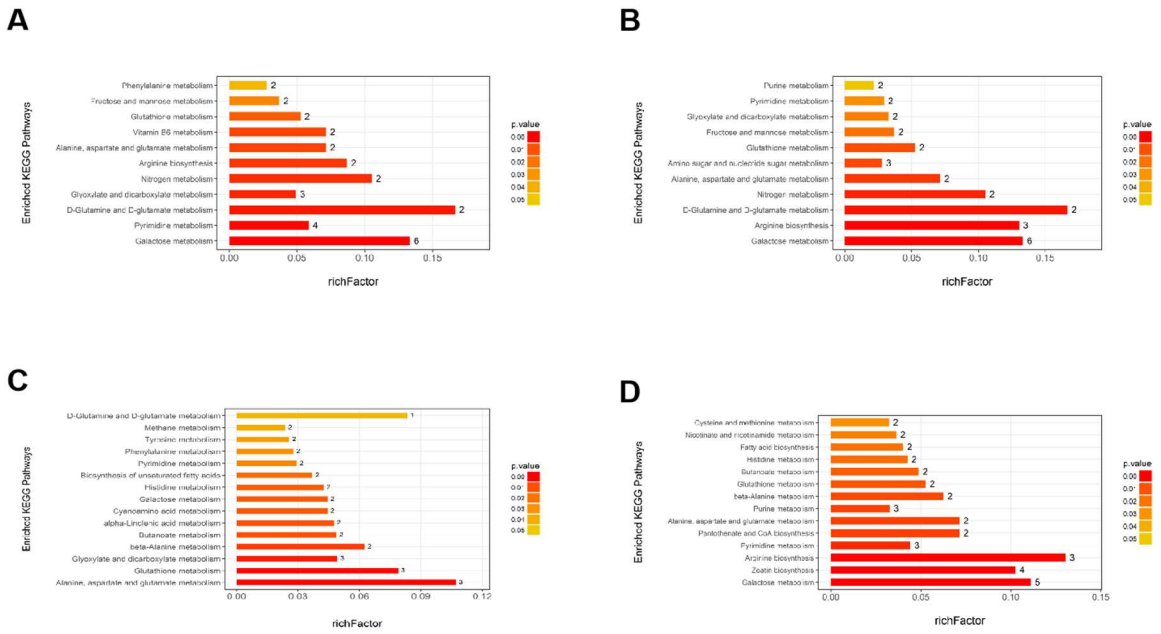


**Figure 9.** Enrichment analysis of differential metabolic entities using the KEGG annotation. (A) FT1-FC (B) FT2-FC(C) FT3-FT1 (D) FT3-FT2.

## 4. Discussion

Climate change is leading to a significant increase in global average temperatures, threatening crop yields and food security. Various strategies have been adopted to enhance the heat tolerance of vegetables and address the dynamic factors that affect modern agricultural production. These strategies include cultivating heat-tolerant varieties, modifying cultivation practices, and increasing $CO_2$ levels. The crops predominantly grown in greenhouses are C3 plants, such as tomatoes and cucumbers, which generally respond more positively to increased $CO_2$ concentrations.[6]. At $CO_2$ levels of 550 to 650 μmol/mol, the yield of C3 crops can increase on average by 18%[23]. Furthermore, at approximately 1000 μmol/mol $CO_2$ concentration, the soluble sugars and certain nutrients in leafy vegetables, fruits and root vegetables can increase from 10% to 60%[24]. Elevated $CO_2$ levels facilitate various physiological activities in C3 crops, including photosynthesis, signaling pathways, and organ development, thereby improving yield, quality, and the resilience of vegetables to abiotic stress[25–27]. This study demonstrates that high temperature conditions inhibit the growth of cucumber fruits while elevated $CO_2$ levels significantly enhance their growth. Specifically, elevated $CO_2$ increases the length and diameter of cucumber fruits under normal and high temperature conditions while also boosting the contents of soluble sugars and vitamin C and notably reducing nitrite levels in the fruits. When comparing a high $CO_2$ environment at normal temperature, the combination of elevated temperature and $CO_2$ concentration markedly improves the number of cucumbers per plant, the weight of each cucumber, and the overall yield per plant, ultimately resulting in the highest harvest volume achieved within the same picking cycle of 35 days. The quality of the fruit aligns more closely with commercial picking standards.

When plants encounter growth-detrimental factors, they rapidly adjust at multiple levels to ensure survival. These responses constitute a complex process that produces mass metabolic intermediates and end products. High-throughput metabolomics elucidates structurally diverse, nutrition-rich metabolites and their intricate interactions within vegetable plants [13]. This approach has facilitated the connection between identified phytometabolites and unique phenotypic traits, nutri-functional characteristics, defense mechanisms, and crop productivity, thus improving our understanding of the principles governing plant life activities at the molecular level. In this study, metabolomics analysis utilizing ultra-high-performance liquid chromatography quadrupole time-of-flight mass spectrometry (UHPLC-Q-TOF MS) revealed significant differences in differential metabolites of greenhouse cucumber fruits under varying temperature and $CO_2$ concentration

 doi:10.20944/preprints202411.1977.v1



conditions. In general, the effect of temperature on the metabolites of the cucumber fruit was more pronounced. In positive and negative ion modes, 58 differential metabolites were identified under FT1-FC, with 20 metabolites unique to FT1-FC. Significantly different metabolites included guanosine, leucylvaline, uridine, isomaltose, xylitol, D-mannose, DL-lactate, heptadecanoic acid, L-threonate, sucrose, myo-inositol, and alpha-D-glucose. Plants utilize various metabolic strategies to cope with heat stress. A study comparing tomato plants (Solanum lycopersicum L.) exposed to temperatures of 45°C and 50°C for one hour daily over seven days against those grown at 25°C revealed a significant positive correlation between heat stress and total phenolic content[28]. Scarano et al. [29]measured β-carotene concentrations in tomato fruits subjected to heat stress conditions in the field, specifically at temperatures exceeding 32°C. The results demonstrated a significant increase in β-carotene concentration in the heat-stressed plants compared to the control group. In this study, cucumber fruits exposed to high-temperature conditions accumulated higher levels of amino acid compounds, such as L-threonate, L-citrulline, and Valine, than those grown under normal conditions. These findings suggest that heat stress may influence the concentration of potentially beneficial nutrients, particularly in fruits.

In the FT2-FC group, 34 differential metabolites were identified, of which 11 were unique to FT2-FC. Significantly different metabolites included dihydroxyacetone, D-mannose, allantoin, and citric acid. Polyols, such as myoinositol, sorbitol, mannitol, and galactitol, are derivatives of sugars. The accumulation of these low molecular weight, uncharged molecules facilitates osmotic adaptation, thereby protecting membrane and cellular proteins from stress. The plant-protective metabolite citric acid, also known as citrate (CA), has emerged as an effective means to enhance plant adaptability to environmental stress, thus maintaining growth and development[30,31]. Alternating oxidase (AOX) can reduce reactive oxygen species levels by enhancing mitochondrial electron transport capacity and inhibiting $O_2^-$ production. Notably, citric acid is the most significant reported inducer of alternating oxidase expression. An increased endogenous citric acid content, whether through in vivo metabolism or exogenous administration, may decrease reactive oxygen species by elevating the activity of alternative oxidases. Foliar spraying of calcium (CA) at a concentration of 200 ppm can effectively mitigate salt stress in eggplant by enhancing plant biomass, pigment levels, primary and secondary metabolites and modulating antioxidant defense systems[32]. Additionally, some studies have indicated that high temperatures influence citrate synthase. Plants can withstand thermal stress by alleviating the denaturation of citrate synthase and promoting the renaturation of the denatured enzyme. Under elevated temperatures, plants enhance mitochondria's heat resistance and improve overall plant heat tolerance by effectively protecting citrate synthase. A related study reported that citric acid accumulates in plants during high-temperature stress, primarily functioning as an antioxidant and an intermediate product of respiratory metabolism, thereby aiding in thermal stress management[33]. Furthermore, spraying of 20 mM CA on leaves of Lolium arundicaceum significantly improved photosynthetic efficiency, Chl biosynthesis, and activity of antioxidant enzymes[34]. This study found cucumber fruits cultivated under normal temperature conditions to scavenge reactive oxygen species by accumulating citrate and related metabolites. However, these metabolites did not exhibit upregulation with increasing $CO_2$ concentrations. This observation suggests that even under normal temperature conditions, enhanced $CO_2$ application can help mitigate stress-induced reactive oxygen damage and improve the stress tolerance of cucumber fruits.

In the FT3-FT1 group, 27 differential metabolites were identified, of which 9 were unique to FT3-FT1. Significant metabolites in this group included tyramine, xylitol, linolenic acid, L-asparagine, alpha-linolenic acid, and L-phenylalanine. In our study, the application of elevated $CO_2$ levels under high-temperature stress resulted in the up-regulation of L-phenylalanine in cucumber fruits. Phenylalanine is a critical substrate in the phenylpropanoid pathway, responsible for synthesizing various compounds, including phenylpropanoids, flavonoids, isoflavones, and anthocyanins [35]. Li et al. demonstrated that the phenylalanine content in cucumber leaves increased significantly under moderate and severe drought stress, suggesting a potential link between drought sensitivity and elevated phenylalanine levels in plant tissues[16,33]. Phenylalanine ammonia-lyase (PAL) catalyzes the deamination of L-phenylalanine into trans-cinnamic acid[34,35]. This pathway generates a range

 doi:10.20944/preprints202411.1977.v1



of aromatic metabolites, such as flavonoids, isoflavones, and lignin [36]. Consequently, PAL plays a vital role in the biosynthesis of multiple secondary metabolites essential for plant growth and development. Beyond its importance in these processes, PAL is also a crucial enzyme in plant stress responses. Its expression is influenced by various factors, including drought [36], pathogen attack, tissue damage, extreme temperatures, ultraviolet radiation, nutrient deficiency[37], and plant signaling molecules such as jasmonic acid (JA) [38], salicylic acid (SA)[39], and abscisic acid (ABA)[40]. After stimulation by different stresses, the expression of the PAL gene is rapidly induced at the transcriptional level [42]. During HT3h (3 hours of heat stress), CsPAL9 was significantly upregulated, while during HT6h (6 hours of heat stress), both CsPAL9 and CsPAL7 exhibited increased expression, indicating their potential involvement in cucumber's tolerance to heat stress[41]. In the future, enhancing the expression of PAL genes may provide a viable strategy to improve plant resistance to various stresses.

In the FT3-FT2 group, 38 differential metabolites were identified, of which 15 were unique to FT3-FT2. Significantly different metabolites included pyridoxal (vitamin B6), L-citrulline, myo-inositol, L-aspartate, MG (16:0), sucrose, D-ribose, and palmitic acid. High temperatures induced alterations in the levels of amino acids, sugars, and organic acid metabolites in cucumber fruits. Amino acids and sugar play a crucial role in the response of higher plants to abiotic stresses. Their derivatives are essential for maintaining intracellular protein structural integrity and osmotic regulation [28,29]. Under heat stress, Arabidopsis and rice accumulate various amino acids, including threonine, isoleucine, leucine, asparagine, malic acid, valine and alanine[30,31]. These findings suggest that the accumulation of metabolites, such as amino acids, sugars, and organic acids, in response to high temperature stress may be vital to adapt cucumber fruits to elevated temperatures.

In response to increased $CO_2$ concentrations under varying temperature conditions, two common differential metabolites were identified in the FT2-FC, FT3-FT1, and FT3-FT2 treatments: L-glutamic acid and stachyose. L-glutamic acid serves as a precursor for chlorophyll a, while the glutamate pathway is the primary source of proline synthesis under osmotic stress[42]. In both normal and high-temperature environments, increased $CO_2$ concentration reduces L-glutamic acid content. This decrease may be attributed to a lowered level of $\alpha$-ketoglutarate, the precursor of glutamate, or to the rise in $CO_2$ concentration that mitigates high-temperature stress, thereby downregulating the typical metabolic response to such stress. Stachyose, a soluble oligosaccharide, is a fuel for growth and development and acts as a precursor and signaling molecule in metabolism. Furthermore, it provides osmotic protection under stress conditions and is integral to the reactive oxygen species (ROS) scavenging system. Stachyose is associated with trehalose metabolism, galactose metabolism, and starch and sucrose metabolism. The accumulation of these carbohydrates in the FC, FT1, and FT2 treatments plays a crucial role in osmotic regulation and protecting cell membranes in cucumber fruits under the corresponding environmental conditions [43].

The enrichment analysis of the KEGG annotation for differential metabolites in cucumber fruit revealed that 11 metabolic pathways were significantly enriched in the FT1-FC group, 11 in the FT2-FC group and 15 in the FT3-FT1 group. In comparison, 14 metabolic pathways were significantly enriched in the FT3-FT2 group. In particular, the galactose metabolism pathway emerged as the most significantly affected pathway in this enrichment analysis. In experiments evaluating the effects of high temperature and elevated $CO_2$ concentration on cucumber fruit quality in greenhouses, the impacts of high temperature and elevated $CO_2$ levels on the soluble sugar and starch content of cucumber fruits were found to be insignificant. However, elevated $CO_2$ concentrations significantly increased the ascorbic acid content in the treatment groups FT2 (17.66±0.68 μg/ml) and FT3 (20.04±0.89 μg/ml) treatment groups. Ascorbic acid (AsA) is an essential redox compound in plant leaves and fruits, playing a critical role in various physiological processes, including the regulation of plant aging [44], protection of photosynthetic structures[45], sugar metabolism[46], and responses to stress. AsA is synthesized primarily in source leaves and transported to storage tissues via the phloem. Plants have an efficient AsA transmembrane and long-distance transport system [47]. Garchery et al. demonstrated that increasing the ascorbic acid (AsA) content in tomato leaves while reducing the activity of ascorbic acid oxidase in tomato fruits can enhance the transport of sucrose

 doi:10.20944/preprints202411.1977.v1



from source leaves to sink tissues, thereby increasing the diameter and yield of transformed tomato fruits [48]. The positive correlation between ascorbic acid (AsA) content and fruit yield can be attributed to the role of AsA in maintaining photosynthesis and respiration [49]. The galactose pathway is the primary pathway for plants to synthesize AsA. High temperature stress significantly alters the response patterns of antioxidant transcription and enzyme activity in cucumber fruits. Following acute oxidative stress, the differential metabolites produced primarily function to maintain or enhance the activity of antioxidant enzymes and mitigate cell membrane lipid peroxidation. Consequently, the galactose metabolism pathway observes a greater abundance of differential metabolites (map00052). The accumulation of cysteine, glutamic acid, and glycine is crucial for synthesizing the antioxidant glutathione. Cucumber fruits in the FT3 group, which maintain a higher amino acid content, exhibit a greater potential to withstand significant high temperature stress. Increased $CO_2$ application complicates metabolic pathways by enriching the changes in differential metabolites of cucumber fruits. Under high-temperature stress, cucumber fruits increase their resistance to stress by accumulating metabolites associated with sugar, organic acids and amino acids, particularly within the galactose metabolism pathway, arginine biosynthesis pathway, and glutamate synthesis pathway.

## 5. Conclusions

Our research indicates that increased $CO_2$ concentration can effectively mitigate the damage caused by high-temperature stress to greenhouse cucumber fruits from a metabolomic perspective. Despite the limited number of studies focusing on plant metabolomic analysis under greenhouse conditions, we believe this is the first study to demonstrate the effects of elevated $CO_2$ application on the metabolomics of greenhouse cucumber fruits subjected to high-temperature stress. We imposed heat stress by varying planting dates to ensure the reproductive period coincided with elevated temperatures. Although there are limitations associated with precise climate control, this experiment holds significant value, as the conditions within an artificial climate chamber may not fully reflect the realities of high-temperature stress experienced in natural settings. It has been reported that crops grown in optimal environments often obscure critical agronomic traits or physiological responses. These findings further underscore the necessity of conducting field experiments to understand the effects of abiotic stresses on vegetable crops. The results of this study offer valuable insights into carbon dioxide fertilization technology and provide a theoretical foundation for utilizing exogenous metabolites to enhance cucumber heat tolerance.

**Supplementary Materials:** Supplementary Figure S1: The OPLS-DA model

**Author Contributions:** Author Contributions: Conceptualization, X.D.and S.C.; methodology, X.D.; investigation, X.D. and Y.S.; data curation, L.P.; writing—original draft preparation, X.D.and Y.S.; writing—review and editing, X.D.and S.C.; visualization, S.C.; supervision, S.C.; funding acquisition, L.P. and S.C. All authors have read and agreed to the published version of the manuscript.

**Funding:** This research was funded by the National Natural Science Foundation of China [31060269], the National Natural Science Foundation of China[31860573], the Research and demonstration project of high-efficiency carbon sequestration technology for facility vegetables[202-202230], the Inner Mongolia Natural Science Foundation Project [2019BS03013], and the" Science and Technology Xingmeng " Action Key Special Funding Project [KJXM-EEDS-2020008].

**Data Availability Statement:** The original contributions presented in the study are included in the article, further inquiries can be directed to the corresponding authors.

**Conflicts of Interest:** The authors declare no conflicts of interest.

## References

1. Argento, S.; Garcia, G.; Treccarichi, S. Sustainable and low-input techniques in mediterranean greenhouse vegetable production. *Horticulturae* **2024**, *10*, 997, doi:10.3390/horticulturae10090997.
2. Francini, A.; Sebastiani, L. Abiotic stress effects on performance of horticultural crops. *Horticulturae* **2019**, *5*, 67, doi:10.3390/horticulturae5040067.

3. Zinati, Z.; Nazari, L. Deciphering the molecular basis of abiotic stress response in cucumber (cucumis sativus L.) using RNA-seq meta-analysis, systems biology, and machine learning approaches. *Sci Rep* **2023**, *13*, 12942, doi:10.1038/s41598-023-40189-3.
4. Heat stress resistance mechanisms of two cucumber varieties from different regions Available online: https://www.mdpi.com/1422-0067/23/3/1817 (accessed on Nov 22, 2024).
5. El-Remaly, E. Morphological, physio-biochemical, and molecular indications of heat stress tolerance in cucumber. *Sci Rep* **2023**, *13*, 18729, doi:10.1038/s41598-023-45163-7.
6. Wang, A.; Lv, J.; Wang, J.; Shi, K. $CO_2$ enrichment in greenhouse production: towards a sustainable approach. *Front. Plant Sci.* **2022**, *13*, doi:10.3389/fpls.2022.1029901.
7. Schapendonk, A.H.C.M.; Van Tilburg, W. The $CO_2$ factor in modelling photosynthesis and growth of greenhouse crops. *Acta Hortic.* **1984**, 83–92, doi:10.17660/ActaHortic.1984.162.7.
8. Du, X. Effects of high temperature and $CO_2$ coupling on physiology, biochemistry, and metabonomics of greenhouse cucumber in the fruiting period. *Inner Mongolia Agricultural University* **2022**, doi:10.27229/d.cnki.gnmnu.2022.001226.
9. Pan, L. Photosynthesis mechanism and proteomics analysis of greenhouse cucumber under high temperature and elevated $CO_2$ coupling. *Inner Mongolia Agricultural University* **2018**.
10. Mashabela, M.D.; Masamba, P.; Kappo, A.P. Metabolomics and chemoinformatics in agricultural biotechnology research: complementary probes in unravelling new metabolites for crop improvement. *Biology* **2022**, *11*, 1156, doi:10.3390/biology11081156.
11. Wedow, J.M.; Yendrek, C.R.; Mello, T.R.; Creste, S.; Martinez, C.A.; Ainsworth, E.A. Metabolite and transcript profiling of guinea grass (panicum maximum jacq) response to elevated $CO_2$ and temperature. *Metabolomics* **2019**, *15*, 51, doi:10.1007/s11306-019-1511-8.
12. Yu, B.; Ming, F.; Liang, Y.; Wang, Y.; Gan, Y.; Qiu, Z.; Yan, S.; Cao, B. Heat stress resistance mechanisms of two cucumber varieties from different regions. *International Journal of Molecular Sciences* **2022**, *23*, 1817, doi:10.3390/ijms23031817.
13. Singh, D.P.; Bisen, M.S.; Shukla, R.; Prabha, R.; Maurya, S.; Reddy, Y.S.; Singh, P.M.; Rai, N.; Chaubey, T.; Chaturvedi, K.K.; et al. Metabolomics-driven mining of metabolite resources: applications and prospects for improving vegetable crops. *International Journal of Molecular Sciences* **2022**, *23*, 12062, doi:10.3390/ijms232012062.
14. Tohge, T.; Fernie, A.R. Metabolomics-inspired insight into developmental, environmental and genetic aspects of tomato fruit chemical composition and quality. *Plant Cell Physiol* **2015**, *56*, 1681–1696, doi:10.1093/pcp/pcv093.
15. Sardans, J.; Gargallo-Garriga, A.; Urban, O.; Klem, K.; Walker, T.W.N.; Holub, P.; Janssens, I.A.; Peñuelas, J. Ecometabolomics for a better understanding of plant responses and acclimation to abiotic factors linked to global change. *Metabolites* **2020**, *10*, 239, doi:10.3390/metabo10060239.
16. Li, M.; Li, Y.; Zhang, W.; Li, S.; Gao, Y.; Ai, X.; Zhang, D.; Liu, B.; Li, Q. Metabolomics analysis reveals that elevated atmospheric $CO_2$ alleviates drought stress in cucumber seedling leaves. *Analytical Biochemistry* **2018**, *559*, 71–85, doi:10.1016/j.ab.2018.08.020.
17. Rangaswamy, T.C.; Sridhara, S.; Manoj, K.N.; Gopakkali, P.; Ramesh, N.; Shokralla, S.; Zin El-Abedin, T.K.; Almutairi, K.F.; Elansary, H.O. Impact of elevated $CO_2$ and temperature on growth, development and nutrient uptake of tomato. *Horticulturae* **2021**, *7*, 509, doi:10.3390/horticulturae7110509.
18. Klopotek, Y.; Kläring, H.-P. Accumulation and remobilisation of sugar and starch in the leaves of young tomato plants in response to temperature. *Scientia Horticulturae* **2014**, *180*, 262–267, doi:10.1016/j.scienta.2014.10.036.
19. Chen, L.; Liang, Z.; Xie, S.; Liu, W.; Wang, M.; Yan, J.; Yang, S.; Jiang, B.; Peng, Q.; Lin, Y. Responses of differential metabolites and pathways to high temperature in cucumber anther. *Front. Plant Sci.* **2023**, *14*, doi:10.3389/fpls.2023.1131735.
20. Gao, B.; Hu, S.; Jing, L.; Niu, X.; Wang, Y.; Zhu, J.; Wang, Y.; Yang, L. Alterations in source-sink relations affect rice yield response to elevated $CO_2$: a free-air $CO_2$ enrichment study. *Front. Plant Sci.* **2021**, *12*, doi:10.3389/fpls.2021.700159.
21. DuBois, Michel.; Gilles, K.A.; Hamilton, J.K.; Rebers, P.A.; Smith, Fred. Colorimetric method for determination of sugars and related substances. *Anal. Chem.* **1956**, *28*, 350–356, doi:10.1021/ac60111a017.
22. López, S.; Maroto, J.V.; San Bautista, A.; Pascual, B.; Alagarda, J. Differences in carbohydrate content of waiting-bed strawberry plants during development in the nursery. *Scientia Horticulturae* **2002**, *94*, 53–62, doi:10.1016/S0304-4238(01)00359-4.
23. Ainsworth, E.A.; Long, S.P. 30 years of free-air carbon dioxide enrichment (FACE): what have we learned about future crop productivity and its potential for adaptation? *Global Change Biology* **2021**, *27*, 27–49, doi:10.1111/gcb.15375.
24. Dong, J.; Gruda, N.; Lam, S.K.; Li, X.; Duan, Z. Effects of elevated $CO_2$ on nutritional quality of vegetables: a review. *Front. Plant Sci.* **2018**, *9*, doi:10.3389/fpls.2018.00924.

25. Ahammed, G.J.; Li, X. Elevated carbon dioxide-induced regulation of ethylene in plants. *Environmental and Experimental Botany* **2022**, *202*, 105025, doi:10.1016/j.envexpbot.2022.105025.
26. Hu, Z.; Ma, Q.; Foyer, C.H.; Lei, C.; Choi, H.W.; Zheng, C.; Li, J.; Zuo, J.; Mao, Z.; Mei, Y.; et al. High $CO_2$- and pathogen-driven expression of the carbonic anhydrase βCA3 confers basal immunity in tomato. *New Phytologist* **2021**, *229*, 2827–2843, doi:10.1111/nph.17087.
27. Xu, Z.; Jiang, Y.; Zhou, G. Response and adaptation of photosynthesis, respiration, and antioxidant systems to elevated $CO_2$ with environmental stress in plants. *Front. Plant Sci.* **2015**, *6*, doi:10.3389/fpls.2015.00701.
28. Alhaithloul, H.A.S.; Galal, F.H.; Seufi, A.M. Effect of extreme temperature changes on phenolic, flavonoid contents and antioxidant activity of tomato seedlings (Solanum lycopersicum L.). *PeerJ* **2021**, *9*, e11193, doi:10.7717/peerj.11193.
29. Scarano, A.; Olivieri, F.; Gerardi, C.; Liso, M.; Chiesa, M.; Chieppa, M.; Frusciante, L.; Barone, A.; Santino, A.; Rigano, M.M. Selection of tomato landraces with high fruit yield and nutritional quality under elevated temperatures. *Journal of the Science of Food and Agriculture* **2020**, *100*, 2791–2799, doi:10.1002/jsfa.10312.
30. El-Tohamy, W.A.; El-Abagy, H.M.; Badr, M.A.; Gruda, N. Drought tolerance and water status of bean plants (Phaseolus vulgaris L.) as affected by citric acid application. *Journal of Applied Botany and Food Quality* **2013**, *86*, doi:10.5073/JABFQ.2013.086.029.
31. Tahjib-Ul-Arif, M.; Zahan, M.I.; Karim, M.M.; Imran, S.; Hunter, C.T.; Islam, M.S.; Mia, M.A.; Hannan, M.A.; Rhaman, M.S.; Hossain, M.A.; et al. Citric acid-mediated abiotic stress tolerance in plants. *International Journal of Molecular Sciences* **2021**, *22*, 7235, doi:10.3390/ijms22137235.
32. Ali, N.; Rafiq, R.; Zaib-un-Nisa; Wijaya, L.; Ahmad, A.; Kaushik, P. Exogenous citric acid improves growth and yield by concerted modulation of antioxidant defense system in brinjal (*solanum melongena* L.) under salt-stress. *Journal of King Saud University - Science* **2024**, *36*, 103012, doi:10.1016/j.jksus.2023.103012.
33. Tahjib-Ul-Arif, Md.; Zahan, Mst.I.; Karim, Md.M.; Imran, S.; Hunter, C.T.; Islam, Md.S.; Mia, Md.A.; Hannan, Md.A.; Rhaman, M.S.; Hossain, Md.A.; et al. Citric Acid-Mediated Abiotic Stress Tolerance in Plants. *Int J Mol Sci* **2021**, *22*, 7235, doi:10.3390/ijms22137235.
34. Hu, L.; Zhang, Z.; Xiang, Z.; Yang, Z. Exogenous application of citric acid ameliorates the adverse effect of heat stress in tall fescue (lolium arundinaceum). *Front. Plant Sci.* **2016**, *7*, doi:10.3389/fpls.2016.00179.
35. Boudet, A.-M. Evolution and current status of research in phenolic compounds. *Phytochemistry* **2007**, *68*, 2722–2735, doi:10.1016/j.phytochem.2007.06.012.
36. Guo, J.; Wang, M.-H. Characterization of the phenylalanine ammonia-lyase gene (SlPAL5) from tomato (solanum lycopersicum L.). *Mol Biol Rep* **2009**, *36*, 1579–1585, doi:10.1007/s11033-008-9354-9.
37. Dixon, R.A.; Achnine, L.; Kota, P.; Liu, C.-J.; Reddy, M.S.S.; Wang, L. The phenylpropanoid pathway and plant defence—a genomics perspective. *Molecular Plant Pathology* **2002**, *3*, 371–390, doi:10.1046/j.1364-3703.2002.00131.x.
38. Khakdan, F.; Alizadeh, H.; Ranjbar, M. Molecular cloning, functional characterization and expression of a drought inducible phenylalanine ammonia-lyase gene (ObPAL) from *Ocimum basilicum* L. *Plant Physiology and Biochemistry* **2018**, *130*, 464–472, doi:10.1016/j.plaphy.2018.07.026.
39. Chen, J.-Y.; Wen, P.-F.; Kong, W.-F.; Pan, Q.-H.; Zhan, J.-C.; Li, J.-M.; Wan, S.-B.; Huang, W.-D. Effect of salicylic acid on phenylpropanoids and phenylalanine ammonia-lyase in harvested grape berries. *Postharvest Biology and Technology* **2006**, *40*, 64–72, doi:10.1016/j.postharvbio.2005.12.017.
40. Jiang, Y.; Joyce, D.C. Aba effects on ethylene production, pal activity, anthocyanin and phenolic contents of strawberry fruit. *Plant Growth Regulation* **2003**, *39*, 171–174, doi:10.1023/A:1022539901044.
41. Amjad, M.; Wang, Y.; Han, S.; Haider, M.Z.; Sami, A.; Batool, A.; Shafiq, M.; Ali, Q.; Dong, J.; Sabir, I.A.; et al. Genome wide identification of phenylalanine ammonia-lyase (PAL) gene family in Cucumis sativus (cucumber) against abiotic stress. *BMC Genomic Data* **2024**, *25*, 76, doi:10.1186/s12863-024-01259-1.
42. Woodward, R.B.; Ayer, W.A.; Beaton, J.M.; Bickelhaupt, F.; Bonnett, R.; Buchschacher, P.; Closs, G.L.; Dutler, H.; Hannah, J.; Hauck, F.P.; et al. The total synthesis of chlorophyll. *J. Am. Chem. Soc.* **1960**, *82*, 3800–3802, doi:10.1021/ja01499a093.
43. Rodziewicz, P.; Swarcewicz, B.; Chmielewska, K.; Wojakowska, A.; Stobiecki, M. Influence of abiotic stresses on plant proteome and metabolome changes. *Acta Physiol Plant* **2014**, *36*, 1–19, doi:10.1007/s11738-013-1402-y.
44. Fotopoulos, V.; Kanellis, A.K. Altered apoplastic ascorbate redox state in tobacco plants via ascorbate oxidase overexpression results in delayed dark-induced senescence in detached leaves. *Plant Physiology and Biochemistry* **2013**, *73*, 154–160, doi:10.1016/j.plaphy.2013.09.002.
45. Tóth, S.Z.; Schansker, G.; Garab, G. The physiological roles and metabolism of ascorbate in chloroplasts. *Physiol Plant* **2013**, *148*, 161–175, doi:10.1111/ppl.12006.
46. Garchery, C.; Gest, N.; Do, P.T.; Alhagdow, M.; Baldet, P.; Menard, G.; Rothan, C.; Massot, C.; Gautier, H.; Aarrouf, J.; et al. A diminution in ascorbate oxidase activity affects carbon allocation and improves yield in tomato under water deficit. *Plant, Cell & Environment* **2013**, *36*, 159–175, doi:10.1111/j.1365-3040.2012.02564.x.

 doi:10.20944/preprints202411.1977.v1



47. Franceschi, V.R.; Tarlyn, N.M. L-Ascorbic acid is accumulated in source leaf phloem and transported to sink tissues in plants. *Plant Physiol* **2002**, *130*, 649–656, doi:10.1104/pp.007062.
48. Garchery, C.; Gest, N.; Do, P.T.; Alhagdow, M.; Baldet, P.; Menard, G.; Rothan, C.; Massot, C.; Gautier, H.; Aarrouf, J.; et al. A diminution in ascorbate oxidase activity affects carbon allocation and improves yield in tomato under water deficit. *Plant Cell Environ* **2013**, *36*, 159–175, doi:10.1111/j.1365-3040.2012.02564.x.
49. Nunes-Nesi, A.; Sulpice, R.; Gibon, Y.; Fernie, A.R. The enigmatic contribution of mitochondrial function in photosynthesis. *J Exp Bot* **2008**, *59*, 1675–1684, doi:10.1093/jxb/ern002.